

# RealCustom++: Representing Images as Real-Word for Real-Time Customization

Zhendong Mao, Mengqi Huang †, Fei Ding, Mingcong Liu, Qian He, Xiaojun Chang, Yongdong Zhang  
Project Page: [https://corleone-huang.github.io/RealCustom\\_plus\\_plus/](https://corleone-huang.github.io/RealCustom_plus_plus/)

**Abstract**—Text-to-image customization, which takes given texts and images depicting given subjects as inputs, aims to synthesize new images that align with both text semantics and subject appearance. This task provides precise control over details that text alone cannot capture and is fundamental for various real-world applications, garnering significant interest from academia and industry. Existing works follow the pseudo-word paradigm, which involves representing given subjects as pseudo-words and combining them with given texts to collectively guide the generation. However, the inherent conflict and entanglement between the pseudo-words and texts result in a dual-optimum paradox, where subject similarity and text controllability cannot be optimal simultaneously. We propose a novel real-words paradigm termed RealCustom++ that instead represents subjects as non-conflict real words, thereby disentangling subject similarity from text controllability and allowing both to be optimized simultaneously. Specifically, RealCustom++ introduces a novel “train-inference” decoupled framework: (1) During training, RealCustom++ learns the alignment between vision conditions and all real words in the text, ensuring high subject-similarity generation in open domains. This is achieved by the cross-layer cross-scale projector to robustly and finely extract subject features, and a curriculum training recipe that adapts the generated subject to diverse poses and sizes. (2) During inference, leveraging the learned general alignment, an adaptive mask guidance is proposed to only customize the generation of the specific target real word, keeping other subject-irrelevant regions uncontaminated to ensure high text-controllability in real-time. Comprehensive experiments demonstrate the superior real-time customization ability of RealCustom++ in the open domain, outperforming existing state-of-the-art methods in both text controllability and subject similarity. Furthermore, we show that RealCustom++ can be effectively extended to various multiple-subject customization tasks.

**Index Terms**—Text-to-image generation, diffusion models, text-to-image customization, attention mechanism, curriculum learning.



## 1 INTRODUCTION

TEXT-to-image customization [1], [2], [3], which simultaneously takes *given texts* and images depicting *given subjects* as inputs, aims to synthesize new images that are consistent with both the *semantics of the texts* and the *appearance of the subjects*. This task allows users to modify specific subjects in provided images using text, such as making your favorite pet wear Iron Man’s suit. Compared to text-to-image generation [4], [5], [6], [7], this task further offers precise control over details that text alone cannot capture (e.g., the unique visual characteristics of your favorite pet), which is crucial for various real-world applications such as film production and personalized recommendations, thereby garnering significant interest from both academia and industry recently. Moreover, this task presents more challenges as its primary goals are dual-faceted: (1) **high subject-similarity**, i.e., the generated subjects should closely mirror *given subjects*; (2) **high text-controllability**, i.e., the remaining subject-irrelevant generated parts should consistently adhere to *given texts*.

Existing text-to-image customization methods follow a two-step **pseudo-word** paradigm: (1) representing the given subjects as pseudo-words [2], [3] that share the same di-

mensionality as real words but are non-existent or meaningless in the vocabulary; (2) combining these pseudo-words with other given texts to guide the generation collectively. According to the different pseudo-words learning ways for subject representation, existing literature can be categorized into finetune-based and encoder-based streams. The former stream [2], [3] adopts the per-subject optimization formulation that finetunes pre-trained text-to-image models [8], [9] to bind the given subject to the pseudo-word. This kind of work either focuses on more efficient finetuning strategies such as finding compact parameter space [10], [11], [12] and extending pseudo-words space [13], [14], [15], [16], or introducing more sophisticated regularization [3], [17], [18] to avoid overfitting. However, this per-subject finetuning requires minutes to hours to learn each subject during inference and over ten reference images containing the same subject to avoid overfitting, which is usually unaffordable for real-world applications. On the contrary, the latter stream [19], [20], [21], [22], [23], [24], [25], [26], which focuses on learning an image encoder to encode the given subject into the pseudo-words, has received more interests since it only requires single forward step and single reference image during inference. These methods focus on developing various adapters [19], [20], [26], [27] to increase the pseudo-word influence for subject-similarity, as well as different regularized losses (e.g.,  $l_1$  penalty [19], [20], [23], alignment loss [25]) to avoid overfitting caused by excessive pseudo-word influence, aiming to maintain a delicate balance. Essentially, existing methods, either the finetune-based

- M. Huang, Z. Mao, X. Chang, Y. Zhang are with the University of Science and Technology of China. E-mail: [huangmq@mail.ustc.edu.cn](mailto:huangmq@mail.ustc.edu.cn), [zdmao,zhyd73@ustc.edu.cn](mailto:zdmao,zhyd73@ustc.edu.cn). Works done during M. Huang’s internship at ByteDance.
- F. Ding, M. Liu, Q. He are with the ByteDance Inc. E-mail: [{dingfei.212,liumingcong,heqian}@bytedance.com](mailto:{dingfei.212,liumingcong,heqian}@bytedance.com).

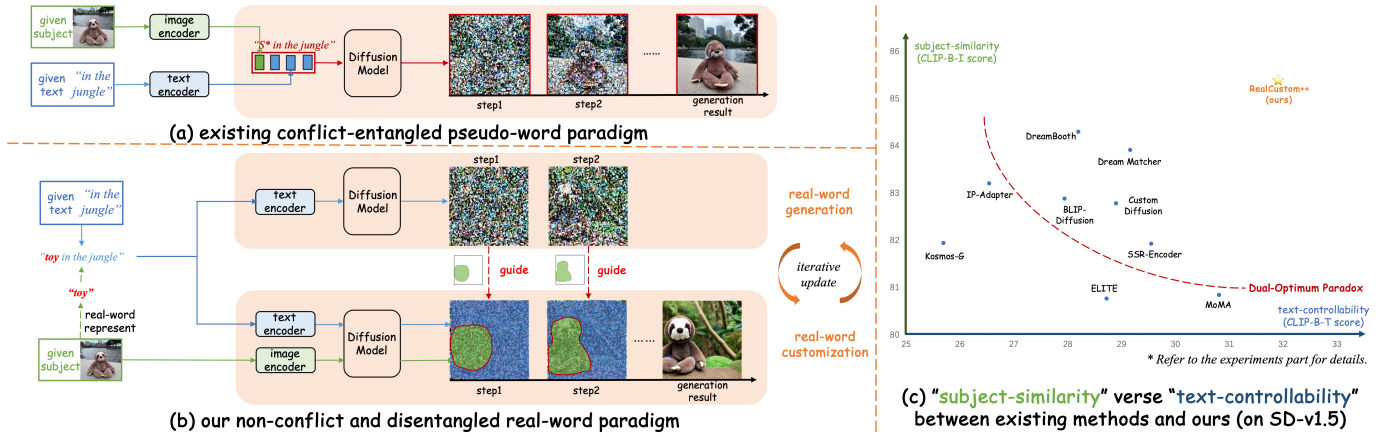


Fig. 1: Illustration of our motivation. (a) Existing paradigm represents the given subject as a **pseudo-word** ( $S^*$ ) and combines it with the given text to collectively guide the generation. The pseudo-word inherently conflicts and entangles with the given text, resulting in the dual-optimum paradox that involves a trade-off between subject-similarity and text-controllability. (b) Our new paradigm, RealCustom++, represents the given subject as a **real-word** ("toy") that integrates seamlessly with the given text. The real-word provides accurate influence masks to guide the given subject at each step, ensuring that the subject only influences within the mask while other regions are controlled purely by the given text, thereby achieving disentanglement. (c) The quantitative comparison shows that RealCustom++ achieves superior similarity and controllability to the existing paradigm.

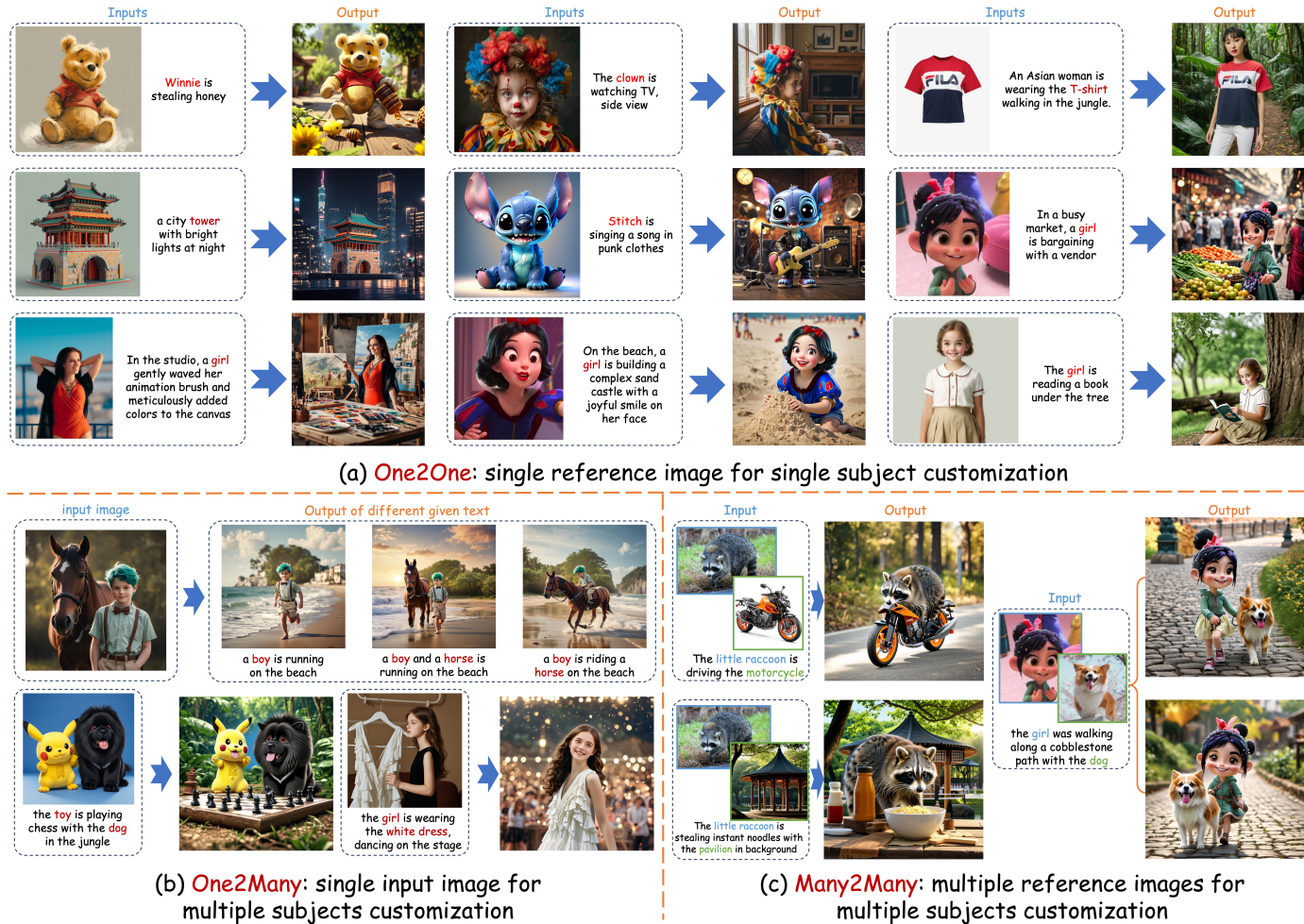


Fig. 2: Our RealCustom++ is naturally capable of various customization tasks. (a) **One2One**: Given a single image depicting the given subject (in open domain, e.g., humans, cartoons, clothes, buildings), RealCustom++ can synthesize images that are consistent with both the semantics of the texts and the appearance of the subjects. (in real-time without any finetuning steps); (b) **One2Many**: RealCustom++ can decouple and customize each subject in a single reference image. (c) **Many2Many**: RealCustom++ can customize multiple subjects from multiple reference images. The customized words are highlighted in color.

or encoder-based, are ensnared in the well-known dual-optimality paradox, where exists a trade-off between subject-similarity and text-controllability and can not achieve the optimum of both simultaneously.

In this study, we argue that the root cause of the dual-optimality paradox lies in the pseudo-word paradigm that integrates pseudo-words representing the given subject with the given text as a unified condition, resulting in inherent conflicts and entanglements between the pseudo-words and the given text. Specifically, (1) conflicts arise from the non-homologous representation between pseudo and real words. Real word representations in pre-trained text-to-image models are learned through large-scale linguistic (e.g., T5 [28]) or multi-modal (e.g., CLIP [29]) pre-training, forming semantically consistent contexts. In contrast, pseudo-word representations are learned by reconstructing input subject images (i.e., visual-only), lacking sufficient interaction with real words. Consequently, pseudo-words are typically meaningless and conflict semantically when combined with real words. Increasing the impact of pseudo-words causes real words to deviate from their original semantics, reducing controllability, while decreasing their impact reduces similarity. (2) Entanglements arise from the overlapping influence scope between the given text and subjects. The unified condition guides generation via built-in cross-attention, updating each image region as the weighted sum of all the pseudo and real words, causing given subjects to indiscriminately influence all regions regardless of relevance. Consequently, increasing the impact of pseudo-words in subject-relevant regions to enhance similarity also amplifies their influence in irrelevant regions, making these regions to adhere to the subject rather than the text, thereby reducing controllability, and vice versa. As a typical generation case shown in Figure 1(a), the existing paradigm unifies the pseudo-word (i.e.,  $S^*$  representing the given sloth toy) and the given text (i.e., "in the jungle") to collectively guide the generation, which results in high subject similarity but low controllability, as the background also closely resembles the input subject images' background and fails to align with the semantics of "in the jungle".

Moreover, the existing pseudo-word paradigm has inherent limitations for open-domain subject customization. It requires explicit correspondence between given subjects and pseudo-words during training, restricting the process to object-level datasets (e.g., OpenImage [30]) with limited categories. Consequently, pseudo-word based methods exhibit poor generalization for real-time, open-domain scenarios.

In this paper, we present **RealCustom++**, a novel customization paradigm that, for the first time, disentangles subject similarity from text controllability and thereby allows both to be optimized simultaneously without any conflicts. Rather than the **existing conflict-entangled paradigm** that represents given subjects as pseudo-words, the core idea of RealCustom++ is to represent given subjects as real words (i.e., its super-category word) that can be seamlessly integrated with given texts, and further leveraging the relevance between real words and image regions to disentangle subjects from texts. Specifically, (1) the conflicts can be fundamentally eliminated since these real words are homologous with the given texts, and (2) the superior text-image alignment of pre-trained text-to-image models allows

these real words to accurately guide the given subject to influence only subject-relevant regions, thereby eliminating entanglement. As illustrated in Figure 1(b), the specific sloth toy is first represented as the real word "toy," which is then integrated with the text "in the jungle" to form the non-conflict condition "toy in the jungle." At each step, this condition generates pure text-guided results with a coherent structure that aim to extract accurate influence mask guidance for the subject. The subject is injected only within the mask, which helps shape a more precise mask for the next step. Through this iterative updating, the generation result of the real word is smoothly and accurately transformed into the subject, while other irrelevant parts are controlled by the text, achieving both high similarity and controllability.

Technically, owing to the absence of annotated paired datasets between "real-words" and "subjects", RealCustom++ introduces an innovative "train-inference" decoupled framework to realize the novel **non-conflict and disentangled real-words paradigm**: (1) During training, RealCustom++ learns the alignment between vision conditions and all real words in the text, ensuring high subject-similarity generation in open domains. This is achieved by the Cross-layer Cross-Scale Projector (CCP) to robustly and finely extract subject features, and a Curriculum Training Recipe (CTR) that adapts the generated subject to diverse poses and sizes. (2) During inference, leveraging the learned general alignment, an Adaptive Mask Guidance (AMG) is proposed to only customize the generation of the specific target real word, keeping other subject-irrelevant regions uncontaminated to ensure high text-controllability in real-time.

Specifically, (1) the CCP module functions in three key steps: (i) Initially, the basic features of the subjects are extracted from the last hidden states of pre-trained image encoders, as these states align well with the original text conditions. (ii) These basic features are enhanced for structural robustness by integrating with shallow hidden states via cross-layer attention and enriched with details through integration with higher-resolution hidden states via cross-scale attention. (iii) Finally, the enhanced features are adaptively fused with the original ones without compromising their initial alignment. The final subject features are incorporated into pre-trained diffusion models by extending textual cross-attention with additional visual cross-attention. (2) The Curriculum Training Recipe (CTR) is designed to align the extracted subject features with all real words in the text, facilitating the generation of open-domain subjects in a variety of poses and sizes with harmonious coherence. This is achieved by introducing a novel "easier-to-harder" subject image data procedure, progressively transitioning the training objective from naive reconstruction to harder re-contextualization. This approach allows the model to converge faster initially and later focus more on aligning with textual semantics, playing a crucial role in bridging the gap between training and inference. (3) During inference, the Adaptive Mask Guidance (AMG) incorporates two distinct branches for each generation step: a Guidance Branch (GuiB) where the visual condition is set to None, and a Generation Branch (GenB) where the visual condition is set to the given subjects. In the GuiB, since cross-attention primarily captures high-level textual semantic correspondences while self-attention captures low-level

per-pixel correspondences, we construct the guidance mask by multiplying the low-resolution cross-attention maps of the target native real words with the high-resolution self-attention maps. In the GenB, the guidance mask from GuiB serves as the influence scope for the given subjects, which is multiplied by the outputs of the visual cross-attention to avoid influencing subject-irrelevant parts. Furthermore, considering the guidance mask tends to converge in the middle diffusion steps and become more scattered later, an “early stop” regularization is proposed for stabilization by reusing previous guidance masks.

We demonstrate that our new paradigm, RealCustom++, is naturally capable of various customization tasks, as illustrated in Figure 2. Given a single image depicting the subject in the open domain, RealCustom++ can generate realistic and harmonious images that consistently adhere to the provided text for the subjects in real-time, without any fine-tuning steps. Moreover, unlike the existing pseudo-word paradigm that learns the correspondence between each pseudo-word and its respective subject, RealCustom++ learns a general alignment between vision conditions and all real words in the text, allowing users to freely select different real words to customize different subjects during inference. Thus, RealCustom++ can naturally extend to multiple subject customizations. For example, RealCustom++ can decouple and customize each subject in a single reference image (i.e., One2Many), as well as customize multiple subjects from multiple reference images (i.e., Many2Many). Both tasks would require additional tedious algorithm design under the existing pseudo-word paradigm.

We summarize our contributions as follows:

**Conceptual Contributions.** For the first time, we (1) identify that the dual-optimum paradox is rooted in the existing pseudo-word paradigm, as it represents subjects as pseudo-words that inherently conflict and entangle with texts; (2) introduce RealCustom++, a novel paradigm that represents subjects as non-conflict real words, thereby disentangling subject similarity from text controllability and allowing both to be optimized simultaneously.

**Technical Contributions.** We propose a novel “train-inference” decoupled framework, which learns the general alignment between vision conditions and all real words in the text during training, and only customizes the generation of the target real word during inference. Specifically,

(i) To improve subject similarity in open domains, a novel Cross-layer Cross-Scale Projector (CCP) is proposed, offering enhanced structural robustness and detail richness; (ii) To better bridge the discrepancy between training and inference, a novel Curriculum Training Recipe (CTR) is designed with an “easier-to-harder” training procedure, adapting generated subjects to diverse poses and sizes. (iii) To improve text controllability in real-time, a novel Adaptive Mask Guidance (AMG) is proposed, featuring a self-attention augmented cross-attention calculation to enhance spatial accuracy and an “early stop” regularization to enhance temporal stabilization.

**Experimental Contributions.** For the first time, we achieve superior subject similarity and text controllability simultaneously for open-domain subjects in real-time scenarios, outperforming existing state-of-the-art customization methods. Moreover, extensive experiments on multiple-

subject customization benchmarks demonstrate the exceptional generalizability of our novel paradigm.

**Extensions.** This manuscript extends RealCustom [31], a conference paper presented at the IEEE/CVF Conference on Computer Vision and Pattern Recognition (CVPR) 2024. Building on the same key idea of representing subjects as non-conflict and disentangled real words introduced in our conference version [31], we completely **redesign our training framework**, enhancing subject similarity by introducing a more structurally robust and detail-rich subject representation and a novel training recipe. In the inference framework, we further **redesign the guidance mask construction algorithm**, leading to more spatially accurate and temporally stable mask guidance. Moreover, we endow it [31] with the **new capability** of multiple subject customization. Specifically, the major extensions include:

**(1) New Training Framework.** (i) **New subject representation learning:** To enhance subject representation for higher subject similarity, we introduce a novel cross-layer attention mechanism designed to improve structural robustness, along with a cross-scale attention mechanism to enrich detail. These mechanisms are then adaptively integrated, ensuring that the original representation’s alignment with the text is preserved. (ii) **New textual alignment learning:** A hand-crafted adaptive scoring module was used in our conference version, requiring manually tuned hyperparameters for optimal generation. We replace it with a novel Curriculum Training Recipe (CTR), which implicitly endows RealCustom++ with the capability to generate given subjects harmoniously in various sizes and poses, thereby eliminating the need for tedious hyper-parameter tuning.

**(2) New Guidance Mask Construction Algorithm during Inference.** The key to text controllability lies in the quality of the guidance mask during inference. Therefore, we redesign the mask construction: (i) **More Spatial Accurate:** We introduce a self-attention augmented cross-attention calculation method, which reduces the noise level of naive cross-attention by incorporating per-pixel correlation. (ii) **More Temporal Stable:** We incorporate an “early stop” regularization to stabilize the guidance mask in later diffusion steps, which also accelerates the generation speed.

**(3) New Capability.** (i) **Advanced backbones:** Previous experiments in our conference version were conducted on SD-v1.5. We further evaluate our paradigm on the more advanced text-to-image backbone model SDXL to thoroughly demonstrate its effectiveness. (ii) **Advanced tasks:** We introduce a new multi-real-words customization algorithm, thereby extending RealCustom++ to accommodate multiple subject customization across various tasks.

## 2 RELATED WORKS

### 2.1 Text-to-Image Customization

Based on the booming research in text-to-image generation [4], [5], [6], [7], [32] and the recent advancements in diffusion models [33], [34], [35], [36], text-to-image customization, which aims to generate text-driven images for subjects specified by users, has garnered rapidly increasing interest. Existing customization methods follow the pseudo-words paradigm, representing given subjects as pseudo-words and then composing them with the given text for customization.

Due to the necessary correspondence between the pseudo-words and the given subjects, existing works are confined to either cumbersome test-time optimization-based methods [2], [3], [10], [12], [13], [15], [16], [37] or optimization-free methods [19], [20], [21], [22], [27], [38] that are trained on object datasets with limited categories.

**Optimization-based customization stream.** In the optimization-based stream, Textual Inversion [2] was the first to propose representing the given subject through new “words” in the embedding space of a frozen text-to-image model. DreamBooth [3] instead used a rare token as the pseudo-word and further fine-tuned the entire pre-trained diffusion model for better similarity. Custom Diffusion [10] proposed finding a subset of key parameters for customization generation (i.e., the key and value projection layer in the diffusion model) and only optimizing them. P+ [15] introduced an extended textual inversion space (i.e., P+), which learns per-layer pseudo-words for faster convergence. Furthermore, NeTI extends the P+ space to P\* space by optimizing to learn separate pseudo-words for each denoising timestep and the denoising U-Net layers. Cones [12] was introduced to optimize residual token embedding for each subject and then compose them through a pre-defined layout. Based on the optimized pseudo-words, many subsequent works [18], [39] further introduce finer image patch features by adding an extra image attention module, significantly improving subject similarity but increasing the risk of overfitting and requiring more regularization mechanisms. The main drawback of this stream is that it requires lengthy optimization time (usually ranging from several minutes to hours) and fine-tuned weights storage for each new subject, bringing excessive computation or memory burden that severely limits their online applications.

**Optimization-free customization stream.** To address the cumbersome requirement of optimizing for each given subject, the optimization-free customization stream has gained increasing research interest recently. Instead of directly optimizing the pseudo-words to represent the given subjects, this stream typically trains an image encoder to project the given subjects into pseudo-words on object-level datasets (e.g., OpenImages [30], FFHQ [40]). ELITE [19] first proposed a learning-based encoder for fast subject customization, consisting of a global mapping network to encode given subjects into pseudo-words and a local mapping network to maintain subject details. BLIP-Diffusion [20] introduces a multimodal encoder for better subject representation, which includes a multimodal encoder pre-training process and a subject representation learning process. InstantBooth [21] proposed rich visual feature representation by introducing a few adapter layers into pre-trained diffusion models, but their method is limited to a few categories (i.e., human, cat, and dog). Subject Diffusion [41] constructs a large-scale dataset consisting of subject detection bounding boxes, segmentation masks, and text descriptions to train the customization model. However, the generated subject usually remains in the same pose as in the reference images and lacks pose diversity, possibly due to their naive reconstruction training objective. More recently, many works [24], [27], [42], [43] focus on human ID-only customized generation. For example, PhotoMaker [42] proposed stacking ID embeddings as the learned pseudo-words

for preserving ID information. InstantID [24] designs an IdentityNet to impose semantic and weak spatial conditions during the training process, integrating facial and landmark images with textual prompts to steer image generation. However, the generated human images also lack subject pose diversity (i.e., the human face can only rigidly face the camera). In summary, these encoder-based works usually show less similarity than optimization-based works and generalize poorly to unseen categories in training.

To conclude, the conflicting semantics and entangled influence scope between foreign pseudo-words and native text limit current methods from achieving both optimal similarity and controllability, hindering real-time open-domain customization.

## 2.2 Multiple subject customization

Though most existing text-to-image customization methods focus on single-subject customization, interest in multiple-subject customization has also increased. The task of multiple-subject customization can be divided into two categories: decoupling multiple given subjects in a single reference image (denoted as One2Many) and learning each given subject in its own reference image and then composing them into one customized result (denoted as Many2Many). Existing methods for multiple-subject customization follow the foreign pseudo-words paradigm used in single-subject customization, i.e., using different pseudo-words to represent each subject and then designing elaborate algorithms to achieve decoupling between different subjects.

**One2Many: decoupling multiple subjects from a single reference image.** Break-a-scene [44] was the first to propose extracting a distinct pseudo-word for each subject by augmenting the input image with masks that indicate the presence of target subjects. The mask is provided by users or generated by a pre-trained segmentation model. Other methods [39], [45] proposed automatic mask generation by using the learned pseudo-words’ corresponding cross-attention mask, either through a fixed threshold or Otsu [46] thresholding. DisenDiff [47] proposes an attention calibration method to distribute attention among different concepts and achieve disentanglement without requiring masks. However, the generated customized results often struggle with the background in the reference images.

**Many2Many: composing multiple subjects from multiple reference images.** This stream customization methods usually focuses on tackling the inter-confusion between different learned subject pseudo-words. Custom Diffusion [10] proposed joint training on multiple concepts and a constrained optimization to merge concepts. However, the optimization process usually requires over ten reference images for each subject to converge. Mix-of-Show [48] adopts an embedding-decomposed LoRA [49] for each subject’s optimization. A similar idea is adopted in MultiBooth [50], where each subject is bounded by pre-defined bounding boxes to define its specific generation area.

To conclude, existing multiple-subject customization research still lags behind single one, as current methods are typically based on optimized single-subject customization formulas. These methods require over ten reference images for each subject and employ various techniques to address

inter-confusion among foreign pseudo-words, making them difficult to apply in real-world scenarios.

### 2.3 Attention in Diffusion Models

Text guidance in modern large-scale text-to-image diffusion models [8], [51], [52], [53], [54] is generally performed using the cross-attention mechanism. Therefore, many works propose manipulating the cross-attention map for text-driven editing [55], [56] on generated images or real images via inversion [57]. For example, Prompt-to-Prompt [55] proposes reassigning the cross-attention weight to edit the generated image. Another branch of work focuses on improving cross-attention either by adding additional spatial control [58], [59] or post-processing to enhance semantic alignment [60], [61]. Meanwhile, several works [62], [63], [64] propose using cross-attention in diffusion models for discriminative tasks such as segmentation. However, unlike the existing literature, the core idea of RealCustom++ is to gradually customize real words from their initial generic concept (e.g., whose cross-attention could represent any toy with various types of shapes and details) to the unique given subject (e.g., whose cross-attention accurately represents the unique toy), which is completely unexplored.

### 2.4 Curriculum Learning

Curriculum learning [65], [66], [67], [68] is a training strategy that organizes the total training data in an “easy-to-hard” manner to train a deep learning model, aiming to imitate the way humans learn curricula. The main purpose of curriculum learning is to improve the final model’s performance on target tasks and speed up the training process, which has been widely applied in neural machine translation [69], entity structure relation extraction [70], etc. Existing curriculum learning methods focus on measuring data difficulty [71], [72], [73], [74] or designing specific training schedulers [75], [76], [77], [78]. However, the application of curriculum learning in image generative tasks remains almost unexplored. Our study fills this gap and shows how to organize and prepare the training data to gradually transition the training of a customization task from a naive “easy” reconstruction objective to a “hard” re-contextualization objective. Such a training process bridges the discrepancy between training and inference, leading to coherent subject generation in diverse poses and sizes.

## 3 METHOD: REALCUSTOM++

In this study, we focus on the most general customization scenario: generating new high-quality images for a given subject based on a single reference image and following the given text. The generated subject may vary in location, pose, style, etc., yet it should maintain high-quality similarity with the reference. The remaining parts of the generated images should consistently adhere to the given text, ensuring high-quality controllability.

We first briefly introduce the preliminaries in Sec. 3.1. The training and inference paradigms of RealCustom++ are elaborated in detail in Sec. 3.2 and Sec. 3.3, respectively. Finally, we illustrate extending our new paradigm to multiple-subject customization tasks in Sec. 3.4.

### 3.1 Preliminaries

Our paradigm is implemented over the popular Stable Diffusion [8], [9], which consists of two components: an autoencoder and a conditional UNet [79] denoiser. Firstly, given an image  $\mathbf{x} \in \mathbb{R}^{H \times W \times 3}$ , the encoder  $\mathcal{E}(\cdot)$  of the autoencoder maps it into a lower-dimensional latent space as  $\mathbf{z} = \mathcal{E}(\mathbf{x}) \in \mathbb{R}^{h \times w \times c}$ , where  $f = H/h = W/w$  is the downsampling factor and  $c$  stands for the latent channel dimension. The corresponding decoder  $\mathcal{D}(\cdot)$  maps the latent vectors back to the image as  $\mathcal{D}(\mathcal{E}(\mathbf{x})) \approx \mathbf{x}$ . Secondly, the conditional denoiser  $\epsilon_\theta(\cdot)$  is trained on this latent space to generate latent vectors based on the text condition  $y$ . The pre-trained CLIP text encoder [29]  $\tau_{\text{text}}(\cdot)$  is used to encode the text condition  $y$  into text features  $\mathbf{f}_{ct} = \tau_{\text{text}}(y)$ . Then, the denoiser is trained with the mean-squared error loss:

$$L := \mathbb{E}_{\mathbf{z} \sim \mathcal{E}(\mathbf{x}), \mathbf{f}_y, \epsilon \sim \mathcal{N}(\mathbf{0}, 1), t} \left[ \|\epsilon - \epsilon_\theta(\mathbf{z}_t, t, \mathbf{f}_{ct})\|_2^2 \right], \quad (1)$$

where  $\epsilon$  denotes for the unscaled noise and  $t$  is the timestep.  $\mathbf{z}_t$  is the latent vector that noised according to:

$$\mathbf{z}_t = \sqrt{\hat{\alpha}_t} \mathbf{z}_0 + \sqrt{1 - \hat{\alpha}_t} \epsilon, \quad (2)$$

where  $\hat{\alpha}_t \in [0, 1]$  is the hyper-parameter that modulates the quantity of noise added. Larger  $t$  means smaller  $\hat{\alpha}_t$  and thereby a more noised latent vector  $\mathbf{z}_t$ . During inference, a random Gaussian noise  $\mathbf{z}_T$  is iteratively denoised to  $\mathbf{z}_0$ , and the final generated image is obtained through  $\mathbf{x}' = \mathcal{D}(\mathbf{z}_0)$ .

The incorporation of text condition in Stable Diffusion is implemented as textual cross-attention:

$$\text{Attention}(\mathbf{Q}, \mathbf{K}, \mathbf{V}) = \text{Softmax}(\mathbf{Q}\mathbf{K}^\top)\mathbf{V}, \quad (3)$$

where the query  $\mathbf{Q} = \mathbf{W}_Q \cdot \mathbf{f}_i$ , key  $\mathbf{K} = \mathbf{W}_K \cdot \mathbf{f}_{ct}$ , and value  $\mathbf{V} = \mathbf{W}_V \cdot \mathbf{f}_{ct}$ . Here,  $\mathbf{W}_Q, \mathbf{W}_K, \mathbf{W}_V$  are the weight parameters of the query, key, and value projection layers.  $\mathbf{f}_i$  and  $\mathbf{f}_{ct}$  are the latent image features and text features, respectively. The latent image feature is then updated with the attention block output.

### 3.2 Training Paradigm

Given a reference image  $\mathbf{x} \in \mathbb{R}^{3 \times H \times W}$ , where  $H$  and  $W$  denote the image height and width, respectively. The reference image is then projected into vision condition  $\mathbf{f}_{ci} \in \mathbb{R}^{n_{\text{image}} \times c_{\text{image}}}$  through the proposed cross-layer cross-scale projector (CCP), where  $n_{\text{image}}$  and  $c_{\text{image}}$  are the vision condition’s token number and dimension. Afterwards, we extend the textual cross-attention in pre-trained diffusion models with an extra visual cross-attention to incorporate the visual condition  $\mathbf{f}_{ci}$ . Specifically, Eq. 3 is rewritten as:

$$\text{Attention}(\mathbf{Q}, \mathbf{K}, \mathbf{V}, \mathbf{K}_i, \mathbf{V}_i) = \text{Softmax}(\mathbf{Q}\mathbf{K}^\top)\mathbf{V} + \text{Softmax}(\mathbf{Q}\mathbf{K}_i^\top)\mathbf{V}_i, \quad (4)$$

where the new key  $\mathbf{K}_i = \mathbf{W}_{K_i} \cdot \mathbf{f}_{ci}$ , value  $\mathbf{V}_i = \mathbf{W}_{V_i} \cdot \mathbf{f}_{ci}$  are added.  $\mathbf{W}_{K_i}$  and  $\mathbf{W}_{V_i}$  are weight parameters. During training, only the CCP module and projection layers  $\mathbf{W}_{K_i}, \mathbf{W}_{V_i}$  in each attention block are trainable, while the weights of other pre-trained models remain frozen. To better align the vision condition with the textual semantics and avoid the training degrading to a naive copy-paste reconstruction, we further propose a curriculum training

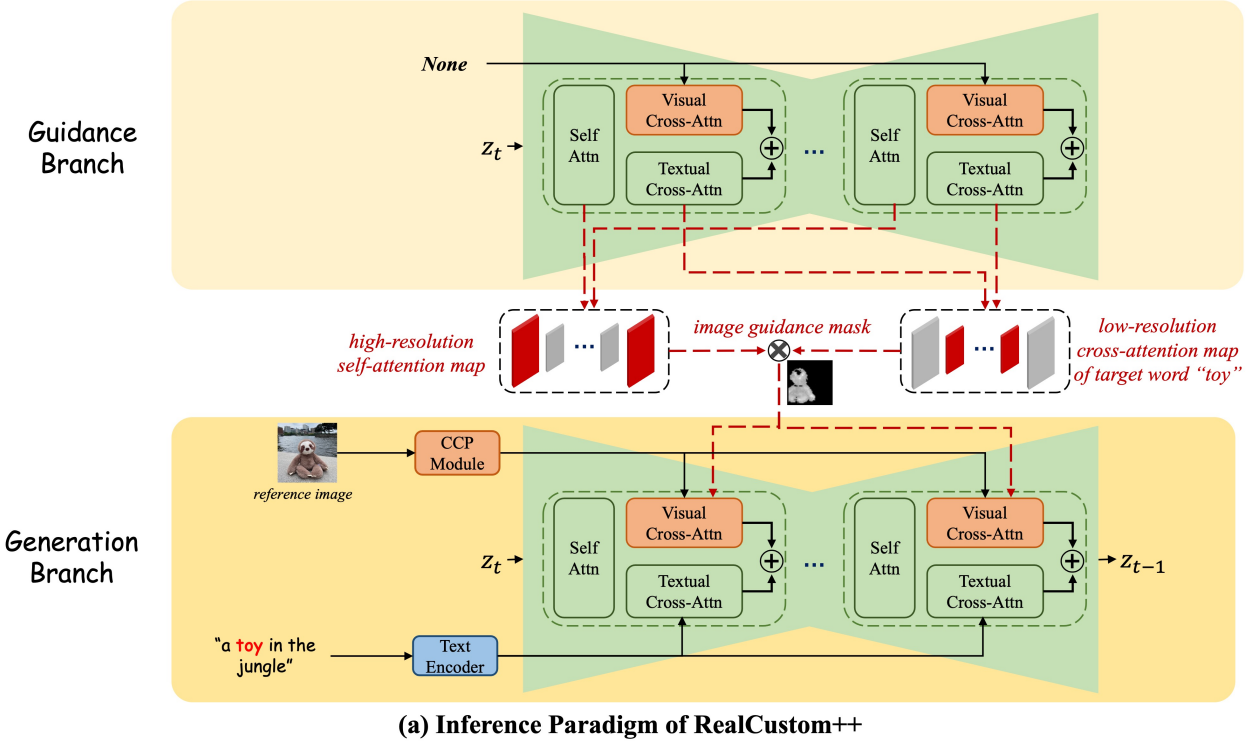
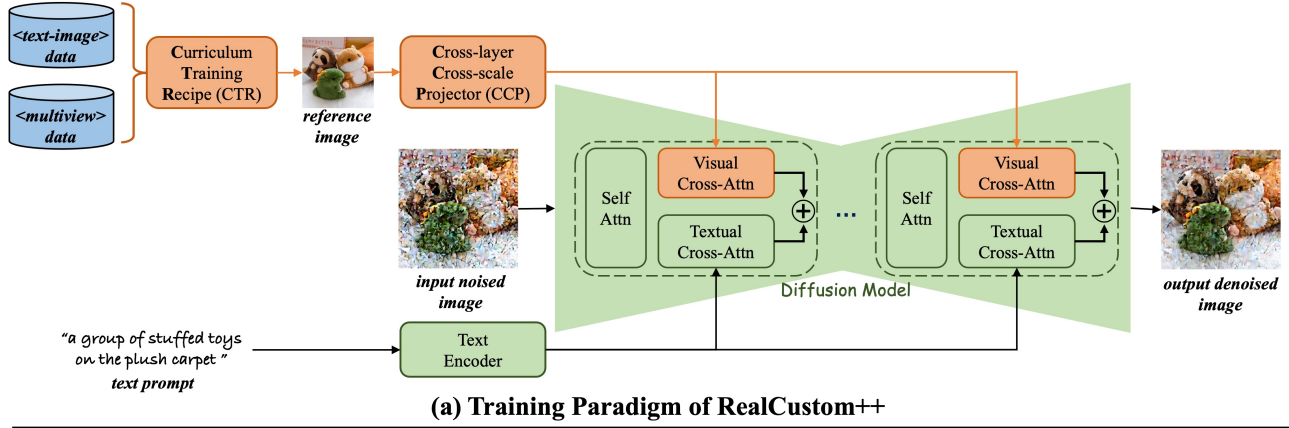


Fig. 3: Illustration of RealCustom++, which employs a novel “train-inference” decoupled framework: (a) During training, RealCustom++ learns the alignment between vision conditions and all real words in the text. This is achieved by the Cross-layer Cross-Scale Projector (CCP) to robustly and finely extract subject features, and a Curriculum Training Recipe (CTR) that adapts the generated subject to diverse poses and sizes. The projected visual conditions are injected into the diffusion models by extending their textual cross-attention with an additional visual cross-attention in each block. (b) During inference, a novel Adaptive Mask Guidance (AMG) strategy is proposed to customize the generation of the specific target real word (“toy” in this case). This is achieved by incorporating two branches for each generation step: a Guidance Branch that constructs the image guidance mask and a Generation Branch that uses the image guidance mask to keep other subject-irrelevant regions uncontaminated.

recipe with a novel “easier-to-harder” subject image data procedure, allowing the subject to be generated in various poses and sizes with harmonious coherence.

### 3.2.1 Cross-layer Cross-scale Projector

In our conference version [31], subject images are encoded from the last hidden states (deep features) of pretrained image ViT encoders, typically CLIP [29] or DINO [80], a standard implementation widely employed by existing customization methods [19], [21], [24], [43]. Given that these image encoders are pretrained with discriminative tasks (e.g., contrastive loss between paired images and text [29] or

self-supervised training [80]), their last hidden states exhibit high semantic richness, providing an advantageous starting point for aligning visual and textual conditions. However, upon further exploration of the model proposed in our conference version across more open-domain unseen subject cases during inference, we identified two key limitations of this prevalent practice:

- (1) **Insufficient structural robustness** Due to the highly semantic nature of deep features, they exhibit limited capacity to preserve low-level shape and structural information, especially for complex subjects (e.g., buildings).
- (2) **Limited detail richness.** Existing common image en-

coders are typically trained for relatively low resolutions (e.g., 224 or 384). Consequently, the given subjects must be resized to these low resolutions, resulting in the loss of numerous subject details.

To address these limitations in existing subject representations, we propose a novel cross-layer cross-scale projector. The key idea is to enhance the subject’s low-resolution deep features with its shallow and high-resolution counterparts, without compromising their initial alignment with the text condition or the efficiency of short token length.

**Cross-layer attention to enhance structural robustness:** Unlike the deep features of the pretrained image encoder, its shallow counterpart contains more low-level structural information [18]. A straightforward solution might be to concatenate the shallow features with the deep ones along the channel dimension. However, our experiments show that this disrupts the original alignment of the deep features, leading to a “copy-paste” issue, as depicted in Figure 5. We hypothesize that shallow features are too low-level and dominate the training process, causing the model to “paste” parts of the reference image directly onto the generated ones. This motivates the design of cross-layer attention, where deep features query shallow ones to enhance structural robustness while maintaining their dominant position.

Mathematically, given the low-resolution deep image features from the last hidden states as  $f_{\text{deep}} \in \mathbb{R}^{n_{\text{image}} \times c_0}$ , we select  $L$  layers of shallow image features denoted as  $f_{\text{shallow}}^l \in \mathbb{R}^{n_{\text{image}} \times c_0}$ , where  $l \in [0, L - 1]$  and  $c_0$  is the dimension of the pretrained image encoder features. These shallow image features are first concatenated along their token dimension as  $f_{\text{shallow}} \in \mathbb{R}^{(n_{\text{image}} \times L) \times c_0}$ , and the cross-layer attention is implemented as

$$f'_{\text{shallow}} = \text{Softmax}(Q^s K^{s\top}) V^s \in \mathbb{R}^{n_{\text{image}} \times c_0}, \quad (5)$$

where  $Q^s = W_{Qs} \cdot f_{\text{deep}}$ ,  $K^s = W_{Ks} \cdot f_{\text{shallow}}$ ,  $V^s = W_{Vs} \cdot f_{\text{shallow}}$ . Here,  $W_{Qs}, W_{Ks}, W_{Vs} \in \mathbb{R}^{c_0 \times c_0}$  are learnable projection matrix. The output features are further projected into the desired dimension as:

$$f'_{\text{shallow}} = \text{MLP}(f_{\text{shallow}}) \in \mathbb{R}^{n_{\text{image}} \times c_{\text{image}}} \quad (6)$$

**Cross-scale attention to enrich subject details.** As depicted in Figure 4, we introduce an additional high-resolution image stream to extract subject representations with enhanced detail. Specifically, we first resize the subject image to twice the target resolution of the pretrained image encoder (e.g.,  $768^2$  for a ViT image encoder [81] pretrained on  $384^2$ ). Subsequently, the high-resolution  $768^2$  subject images are partitioned into four  $384^2$  local images, which are then fed into the pretrained image encoder. These local image features are concatenated along their token dimension, yielding a quadruple-length feature  $f_{\text{high}} \in \mathbb{R}^{(4 \times n_{\text{image}}) \times c_0}$ . Directly using these quadruple-length features significantly increases the training cost (i.e., experimentally, the maximum batch size is limited to 1 when directly feeding these features into the visual cross-attention). Another cross-scale attention is implemented to integrate the high-resolution local features with the original low-resolution global features without increasing the token length:

$$f'_{\text{high}} = \text{Softmax}(Q^h K^{h\top}) V^h \in \mathbb{R}^{n_{\text{image}} \times c_0}, \quad (7)$$

where  $Q^h = W_{Qh} \cdot f_{\text{deep}}$ ,  $K^h = W_{Kh} \cdot f_{\text{high}}$ ,  $V^h = W_{hv} \cdot f_{\text{high}}$ . Here,  $W_{Qh}, W_{Kh}, W_{hv} \in \mathbb{R}^{c_0 \times c_0}$  are learnable projection matrices. Similarly,

$$f'_{\text{high}} = \text{MLP}(f_{\text{high}}) \in \mathbb{R}^{n_{\text{image}} \times c_{\text{image}}} \quad (8)$$

**Feature combination.** After acquiring the structural-enhanced features  $f'_{\text{shallow}}$  and the detail-enhanced features  $f'_{\text{high}}$ , we propose to combine these features with the original low-resolution deep features  $f_{\text{deep}}$  using token-wise concatenation and element-wise addition, respectively:

$$f_{ci} = f'_{\text{shallow}} \oplus (\text{MLP}(f_{\text{deep}}) \oplus f'_{\text{high}}) \in \mathbb{R}^{n_{\text{image}} \times c_{\text{image}}}, \quad (9)$$

where MLP denotes the multi-layer perceptrons that project  $f_{\text{deep}}$  to the desired output dimension  $c_{\text{image}}$ .  $\oplus$  and  $\oplus$  denote token-wise concatenation and element-wise addition, respectively. The design rationale is that  $f'_{\text{high}}$  shares the same level features (i.e., the semantically rich last hidden states) and thus element-wise addition will not cause conflicts, while  $f'_{\text{shallow}}$  contains different level features, and thus token-wise concatenation allows the model to adaptively select different level information in Eq. 4.

### 3.2.2 Curriculum Training Recipe

The key to open-domain subject customization lies in training the model on open-vocabulary datasets, ensuring its generalizability to unseen subjects. In our conference version, we trained the model on the generic `<text-image>` dataset (i.e., Laion-5B [83]), where the same images served both as the visual conditions and inputs to the diffusion denoiser. However, this approach led to a “train-inference” gap: during training, the generated subject has the same pose and size as the one in the reference images, while during inference, the generated subjects should adaptively generalize to various poses and sizes for different text prompt cases. As evidenced by many recent milestone studies [9], [84] in generative models, the preparation of training data plays a vital role in final generation performance. For example, one of the key contributions of Stable Video Diffusion [84] lies in their data selection and curation recipe. In this paper, we also emphasize that an appropriate training data setting is crucial for consistent high-quality customization. As illustrated in Figure 6, we present a novel curriculum training recipe that enables the model to implicitly learn to customize subjects in a variety of coherent poses and sizes without specific model designs.

**Adaption to diverse subject pose.** We propose to expand the training data used in our conference version [31] to a mix of the generic `<text-image>` dataset (i.e., Laion [83]) and the `<multiview>` dataset (i.e., MVImageNet [82]). The former encompasses a wide range of open-domain subjects but lacks diversity in subject poses and views, while the latter provides various poses and views for each subject but is limited to a narrow range of categories (i.e., 238 classes primarily comprising daily necessities, but lacking cartoon characters, humans, animals, buildings, etc.). We propose to progressively increase the proportion of `<multiview>` data while concurrently decreasing the `<text-image>` data. This approach initially exposes the model to a broader



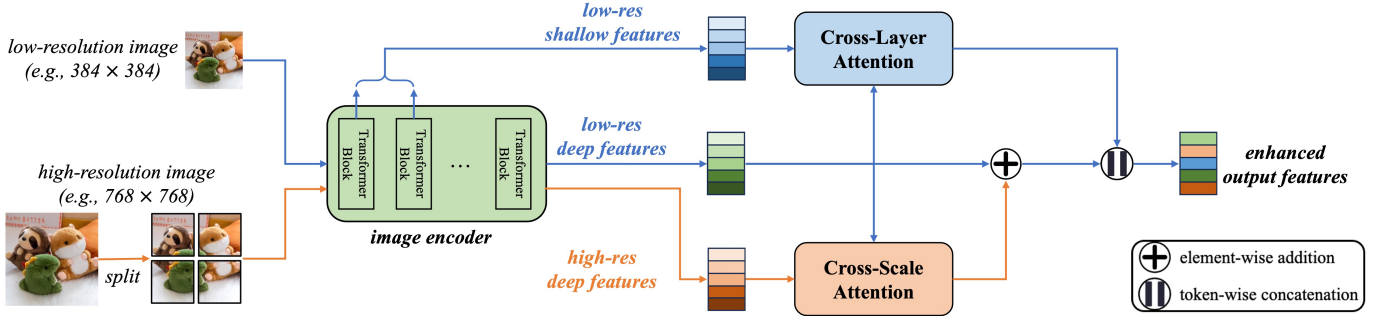


Fig. 4: Illustration of the proposed Cross-Layer Cross-Scale Projector.



Fig. 5: Illustration of a typical failure when naively concatenating shallow features with deep ones, resulting in a “copy-paste” problem that disrupts the alignment between text and deep image features.

Fig. 7: Illustration of typical failure cases of training without subject size adaptation, resulting in incoherence between subject regions and other purely text-controlled, subject-irrelevant regions. This incoherence often manifests as disproportionate figures, such as a “large head with a small body” or “half body.”

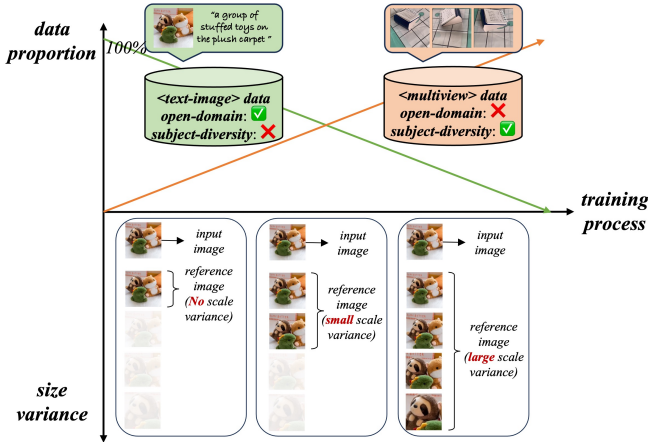


Fig. 6: The illustration of the proposed curriculum training recipe (CTR). To enhance pose diversity and maintain open-domain generation, RealCustom++ is trained on a mix of generic <text-image> data and <multiview> data [82]. We progressively adjust the dataset proportions, initially favoring open-domain data and later augmenting pose generalization. Concurrently, the model is gradually trained with reference images of increasing size variance, promoting initial fast convergence and later subject size generalization.

range of open-domain data, facilitating rapid convergence and generalization to all kinds of subjects, as the model primarily performs a naive reconstruction task. By gradually increasing the <multiview> data proportion, we incrementally increase the complexity of the model’s training tasks from naive reconstruction to diverse view synthesis, thereby enhancing its adaptability to diverse subject poses without compromising its open-domain generalization.

Specifically, given the total training steps  $S_{total}$  and the

current training step  $S_{cur}$ , the probability of using the <text-image> dataset and <multiview> data for the current training step is  $P_{cur}^{generic}$  and  $P_{cur}^{multiview}$ , respectively:

$$P_{cur}^{multiview} = \frac{S_{cur}}{S_{total}}, \quad (10)$$

$$P_{cur}^{generic} = 1 - P_{cur}^{multiview}. \quad (11)$$

**Adaption to diverse subject size.** Despite the enhancement in model adaptability to diverse subject poses and views through training with multiview data, we still observe some failure cases characterized by incoherent generation between subject regions and other text-controlled, subject-irrelevant regions. This incoherence often manifests as disproportionate figures, such as a “large head with a small body” or “half body”, as shown in Figure 7. We hypothesize that this issue arises due to the model’s inability to generate various sizes of a given subject that significantly deviate from the size in the reference image (i.e., generating a very small head when provided with a reference image featuring a very large head). Hence, we propose a gradual training approach with reference images exhibiting increased size variance. This strategy promotes faster and more stable convergence initially, and better size generalization subsequently. Specifically, for a reference image with a resolution of  $384^2$ , we implement a random cropping strategy with incrementally increasing intervals:

$$r_{\text{cur}} = r_{\text{min}} + (r_{\text{max}} - r_{\text{min}}) \times \frac{S_{\text{cur}}}{S_{\text{total}}}, \quad (12)$$

$$r_{\text{sample}} \sim U(r_{\text{min}}, r_{\text{cur}}), \quad (13)$$

where  $S_{\text{cur}}$  denotes the current training steps and  $S_{\text{total}}$  denotes the total training steps. The terms  $r_{\text{min}}, r_{\text{max}}, r_{\text{cur}}$  denote the minimum, maximum, and current image resize ratios, respectively. A random ratio  $r_{\text{sample}}$  is sampled for each training step from a uniform distribution  $U(r_{\text{min}}, r_{\text{cur}})$ . Subsequently, we first resize the reference image to  $(384 \times r_{\text{sample}})^2$  and then randomly crop a  $384^2$  patch from it. This patch serves as the final reference image, which is fed into the image projector to extract image features. Empirically, we set  $r_{\text{min}} = 1.0$  and  $r_{\text{max}} = \sqrt{10}$ , resulting in the most extreme case where the randomly cropped patch constitutes a minimum of 10% of the original reference image’s area.

### 3.3 Inference Paradigm

As depicted in Figure 3(b), the inference paradigm of RealCustom++ comprises two branches at each generation step: a Guidance Branch (GuiB), where the visual condition is set to None, and a Generation Branch (GenB), where the visual condition corresponds to the given subjects. These two branches are interconnected by our proposed Adaptive Mask Guidance (AMG) strategy. Specifically, given the output  $z_t$  from the previous step, GuiB first performs a pure text-conditional denoising process to obtain the guidance mask, which is subsequently utilized in GenB.

#### 3.3.1 Guidance Branch

**More spatially accurate image guidance mask:** On one side, the textual cross-attention in pre-trained diffusion models primarily captures high-level textual semantic correspondences. Consequently, low-resolution cross-attention maps tend to be more focused and less noisy, while high-resolution cross-attention maps are the opposite. On the other side, self-attention primarily captures low-level per-pixel correspondences, resulting in a high-resolution self-attention map that is more fine-grained and thus more accurate. Therefore, considering their strengths and weaknesses, we propose constructing a more spatially accurate image guidance mask than our conference version [31] by multiplying the low-resolution cross-attention maps of the target native real words (e.g., the real word “toy” in Figure 3(b)) with the high-resolution self-attention maps in the GuiB. Specifically, we first extract and resize all low-resolution cross-attention maps of the target native real words to the largest map size (e.g.,  $64 \times 64$  in Stable Diffusion XL), denoted as  $M_{\text{cross}} \in \mathbb{R}^{64 \times 64}$ .  $M_{\text{cross}}$  is further expanded to 1D as  $M_{\text{cross}} \in \mathbb{R}^{(64 \times 64) \times 1}$ . Then, we extract and resize all high-resolution self-attention maps to  $M_{\text{self}} \in \mathbb{R}^{4096 \times 4096}$ . The multiplied attention map is denoted as  $M$ :

$$M = M_{\text{self}} M_{\text{cross}} \in \mathbb{R}^{4096 \times 1}, \quad (14)$$

which is then re-expanded to 2D as  $M \in \mathbb{R}^{64 \times 64}$ . Next, a Top-K selection is applied: given the target ratio  $\gamma_{\text{scope}} \in [0, 1]$ , only  $\lceil \gamma_{\text{scope}} \times 64 \times 64 \rceil$  regions with the highest attention scores are retained, while the rest are set to zero.

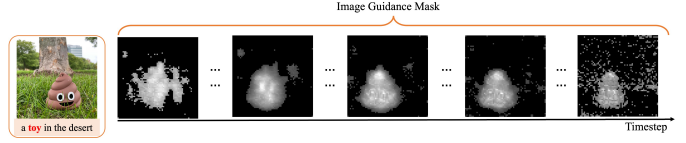


Fig. 8: Illustration of the motivation behind the early stop regularization for mask calculation, where the image guidance mask tends to converge in the middle diffusion steps and become more scattered in the later steps.

The selected attention map  $\bar{M}$  is then normalized by its maximum value as:

$$\hat{M} = \frac{\bar{M}}{\max(\bar{M})}, \quad (15)$$

where  $\max(\cdot)$  represents the maximum value. The rationale for this normalization, rather than simply setting it to binary, is that even within these selected parts, their subject relevance varies. Therefore, different regions should have different weights to ensure smooth generation results between masked and unmasked regions.

**More temporally stable image guidance mask:** Through experimentation, we discovered that as the generation process advances, the image guidance mask tends to converge in the middle diffusion steps and become more scattered later, as illustrated in Figure 8. Consequently, we propose an “early stop” regularization to stabilize the guidance mask in these later stages. Specifically, given a timestep threshold  $T_{\text{stop}}$ , we reuse the image guidance mask  $\hat{M}_{T_{\text{stop}}}$  for diffusion steps later than  $T_{\text{stop}}$ . This regularization strategy not only stabilizes the image guidance mask for the latter diffusion steps but also accelerates the customization process, as only a single GenB branch is required after  $T_{\text{stop}}$ .

#### 3.3.2 Generation Branch

In the GenB, the influence scope  $\hat{M}$  is multiplied by the visual cross-attention results to mitigate any negative impacts on the controllability of the given texts in other subject-irrelevant regions. Specifically, Eq. 4 is reformulated as:

$$\text{Attention}(Q, K, V, K_i, V_i) = \text{Softmax}(QK^\top)V + \text{Softmax}(QK_i^\top)V_i\hat{M}, \quad (16)$$

where the necessary resize operation is applied to match the size of  $\hat{M}$  with the resolution of each cross-attention block. The denoised output of GenB is denoted as  $z_{t-1}$ . Classifier-free guidance [85] is applied to produce the next step’s denoised latent feature  $z_{t-1}$  as:

$$z_{t-1} = \epsilon_\theta(\emptyset) + \omega(z_{t-1} - \epsilon_\theta(\emptyset)), \quad (17)$$

where  $\epsilon_\theta(\emptyset)$  is the unconditional denoised output and  $\omega$  is the classifier-free guidance strength.

### 3.4 Extension To Multi-subjects Customization

In contrast to the existing pseudo-word paradigm, which learns the correspondence between each pseudo-word and its respective subject, RealCustom++ establishes a general alignment between vision conditions and all real words in

the text during training. This allows users to freely select different real words to customize various subjects during inference. This inherent flexibility makes RealCustom++ readily extendable to multiple-subject customization.

**Extension to decouple multiple subjects from a single reference image (One2Many).** Unlike previous foreign pseudo-word paradigm methods that require region-wise attention regularization or pre-defined masks to separate multiple subjects within a single reference, RealCustom++ can accomplish this task without any additional design: simply utilize different native real words to represent the target subjects in the reference images. As illustrated in Figure 2(b), using ‘boy’ to customize only the target boy with green hair or simultaneously using ‘boy’ and ‘horse’ to customize both subjects, the disentanglement is naturally achieved thanks to the well-learned alignment between vision conditions and original text conditions.

**Extension to compose multiple subjects from multiple reference images (Many2Many).** Given  $N$  reference images, each representing a different subject, we extend the Top-K selection to the Multi-Subject Top-K selection as illustrated in Alg.1. The key is to iteratively select the maximum scores for each given subject while ensuring that these guidance masks do not overlap. After acquiring the selected attention map for each subject  $\bar{M}_j, j \in [0, N - 1]$ , maximum normalization is applied to each:

$$\hat{M}_j = \frac{\bar{M}_j}{\max(\bar{M})_j}, j \in [0, N - 1]. \quad (18)$$

Then the Eq. 16 is rewritten as:

$$\text{Attention}(\mathbf{Q}, \mathbf{K}, \mathbf{V}, \mathbf{K}_i, \mathbf{V}_i) = \text{Softmax}(\mathbf{Q}\mathbf{K}^\top)\mathbf{V} + \sum_{j=0}^{N-1} \text{Softmax}(\mathbf{Q}\mathbf{K}_i^j{}^\top)\mathbf{V}_i^j\hat{M}_j, \quad (19)$$

where  $\mathbf{K}_i^j, \mathbf{V}_i^j$  stand for the projected vision key and value for  $j^{\text{th}}$  reference image, respectively.

## 4 EXPERIMENTS

We first describe our experimental setups in Section 4.1. Then, we compare our proposed RealCustom++ with state-of-the-art customization methods in Section 4.2 to demonstrate its superiority in subject similarity and text controllability. Finally, the ablation study of each component of RealCustom++ is presented in Section 4.3.

### 4.1 Experimental Setups

**Implementation Details.** RealCustom++ is implemented based on the pretrained Stable Diffusion 1.5 [8] and Stable Diffusion XL [9] to further validate the generalization. We use a mix of the generic <text-image> dataset (i.e., the filtered subset of Laion-5B [83] based on aesthetic score) and the <multi-view> dataset (i.e., MVImageNet [82]) as detailed in Sec.3.2.2. RealCustom++ is trained using 8 A100 GPUs for 160,000 iterations with a learning rate of  $1e-4$ . For Stable Diffusion XL, we first train the model at a 512 resolution for 60,000 iterations and then further fine-tune it at a 1024 resolution for another 100,000 iterations.

---

### Algorithm 1 Guidance Mask Construction Algorithm for Multiple Subjects Customization.

---

**Input:** given subject number  $N$ , the multiplied map before selection for each subject  $M_j, i \in [0, N - 1]$ , the target ratio for each subject  $\gamma_{\text{scope}}, j \in [0, N - 1]$ .

**Output:** the selected attention map for each subject  $\bar{M}_j, j \in [0, N - 1]$ .

- 1:  $\gamma_{\text{num}} = \lfloor \gamma_{\text{scope}} \times 64 \times 64 \rfloor$ , where  $j \in [0, N - 1]$ ;
- 2:  $\gamma_{\text{current}} = 0$ , where  $j \in [0, N - 1]$ ;
- 3:  $\mathbf{M}_j = \mathbf{0}, j \in [0, N - 1]$ ;
- 4:  $\mathbf{M}_{\text{flag}} = \mathbf{0}$  {A flag mask that denotes whether a position has been allocated to a given subject, 1 denotes for allocated};
- 5: **while**  $\sum_j^{N-1} (\gamma_{\text{current}} < \gamma_{\text{num}})$  **do**
- 6:   **for**  $j = 0$  to  $N - 1$  **do**
- 7:     **if**  $\gamma_{\text{current}} < \gamma_{\text{num}}$  **then**
- 8:       Set\_NegInf( $\mathbf{M}_j, \mathbf{M}_{\text{flag}}$ ) {For positions in  $\mathbf{M}_{\text{flag}}$  that are 1, the corresponding values in  $\mathbf{M}_j$  are set to negative infinity to avoid repeat selection};
- 9:       ( $h, w$ ) = Copy\_Top1( $\bar{M}_j, \mathbf{M}_j$ ) {Copy the maximum value in  $\mathbf{M}_j$  to the corresponding position in  $\bar{M}_j$ , ( $h, w$ ) is the position of the maximum value};
- 10:       Set\_Flag( $(h, w), \mathbf{M}_{\text{flag}}$ ) {set the value of the position ( $h, w$ ) in  $\mathbf{M}_{\text{flag}}$  to 1};
- 11:        $\gamma_{\text{current}} = \gamma_{\text{current}} + 1$
- 12:     **end if**
- 13:   **end for**
- 14: **end while**

---

We use SigLip [81] and DINO [80] with a  $384^2$  input image size as our image encoders, concatenating their last hidden states in the channel dimension to formulate the deep image features  $\in \mathbb{R}^{729 \times 2176}$ . Therefore, the notation  $n_{\text{image}} = 729$  and  $c_{\text{image}} = 2176$ . The shallow layer number  $L = 3$ , and the selected shallow layers for SigLIP and DINO are  $\{7, 13, 19\}$  and  $\{4, 10, 16\}$ , respectively. These layers are also concatenated in the channel dimension correspondingly, resulting in triple-level shallow image features. Unless otherwise specified, for Stable Diffusion 1.5, the DDIM sampler [57] with 50 sample steps is used for sampling, and the classifier-free guidance  $\omega$  is set to 12.5. For Stable Diffusion XL, the DDIM sampler [57] with 25 sample steps is used for sampling, and the classifier-free guidance  $\omega$  is set to 7.5. The Top-K ratio  $\gamma_{\text{scope}}$  is set to 0.2 by default. The timestep threshold  $T_{\text{stop}}$  for mask calculation early stop regularization is set to 25 for SD-v1.5 and 12 for SDXL.

**Evaluation Metrics.** We comprehensively evaluate our proposed RealCustom++ using various standard automatic metrics for subject similarity and text controllability.

**(1) Subject-Similarity:** We use the state-of-the-art segmentation model, SAM [92], to segment the subject, and then evaluate with both CLIP-I and DINO [80] scores. These scores represent the average pairwise cosine similarity of CLIP or DINO embeddings of the segmented subjects in generated and given images. For a more robust evaluation, we adopt two variants of CLIP: CLIP ViT-B/32 (denoted as CLIP-B-I) and CLIP ViT-L/14 (denoted as CLIP-L-I).

**(2) Text-Controllability:** We calculate the cosine similarity between the prompt and the image CLIP embeddings (CLIP-T). Similarly, two variants of CLIP are adopted: CLIP ViT-B/32 (denoted as CLIP-B-T) and CLIP ViT-L/14 (denoted as CLIP-L-T). Moreover, ImageReward [93] (denoted as IR) is also used to evaluate both text controllability and

Method	BaseModel	text controllability			subject similarity		
		CLIP-B-T↑(%)	CLIP-L-T↑(%)	IR↑	CLIP-B-I↑(%)	CLIP-L-I↑(%)	DINO-I↑(%)
DreamBooth <sub>2023</sub> [3]	SD-v1.5	28.20	23.91	0.1856	84.29	83.22	71.31
Custom Diffusion <sub>2023</sub> [10]	SD-v1.5	28.94	25.29	<u>0.2401</u>	82.78	81.54	68.42
DreamMatcher <sub>2024</sub> [17]	SD-v1.5	29.16	25.37	0.2209	83.91	82.85	69.11
ELITE <sub>2023</sub> [19]	SD-v1.5	28.72	25.07	-0.0527	80.76	78.92	66.86
BLIP-Diffusion <sub>2024</sub> [20]	SD-v1.5	27.94	24.32	-0.6376	82.88	80.93	67.38
IP-Adapter <sub>2023</sub> [43]	SD-v1.5	26.54	22.63	-0.6199	83.20	81.56	68.00
Kosmos-G <sub>2024</sub> [86]	SD-v1.5	25.69	21.26	-0.5177	81.94	80.20	65.24
MoMA <sub>2024</sub> [87]	SD-v1.5	<u>30.81</u>	<u>26.75</u>	0.1697	80.84	79.16	66.73
SSR-Encoder <sub>2024</sub> [88]	SD-v1.5	29.55	25.72	0.0768	81.92	79.58	67.13
<b>RealCustom++(ours)</b>	SD-v1.5	<b>31.92</b>	<b>28.72</b>	<b>0.7628</b>	<b>86.36</b>	<b>84.16</b>	<b>73.14</b>
Custom Diffusion <sub>2023</sub> [10]	SDXL	30.87	28.49	<u>0.6255</u>	85.01	84.11	69.79
IP-Adapter <sub>2023</sub> [43]	SDXL	29.74	27.32	0.1807	84.93	83.02	69.43
Emu-2 <sub>2024</sub> [89]	SDXL	26.34	22.01	-0.4293	83.33	82.19	67.32
λ-ECLIPSE <sub>2024</sub> [90]	Kandinsky v2.2	27.19	22.87	-0.3876	84.60	83.21	68.62
MS-Diffusion <sub>2024</sub> [91]	SDXL	<u>31.24</u>	<u>29.03</u>	0.5522	82.84	82.01	69.33
<b>RealCustom++(ours)</b>	SDXL	<b>33.43</b>	<b>31.20</b>	<b>1.1036</b>	<b>87.32</b>	<b>86.67</b>	<b>74.60</b>

TABLE 1: Quantitative comparisons. RealCustom++ outperforms existing methods across all metrics on both SD-v1.5 and SDXL. Specifically: (1) For text controllability, on the more powerful base model SDXL, we achieve improvements of 7.01%, 7.48%, and 76.43% on CLIP-B-T, CLIP-L-T, and ImageReward, respectively. The significant improvement on ImageReward validates that RealCustom++’s non-conflict subject representation and the disentangled influence scope between texts and subjects can generate customized images with much higher quality (higher aesthetic score), as other subject-irrelevant regions are completely controlled by the given text without contamination from the subjects. (2) For subject similarity, we achieve state-of-the-art performance on CLIP-B-I, CLIP-L-I, and DINO-I, validating that RealCustom++ can generate more similar subjects in the subject-relevant regions.

aesthetics (image generation quality).

**Evaluation Benchmarks.** Following previous works, we use the prompt “a photo of [category]” to generate images for calculating similarity. The full editing prompts and subject images used for evaluation are provided in the Appendix. These editing prompts and subject images are derived from the standard DreamBench [3] and are further supplemented with more challenging cases in open domains, such as cartoon characters and buildings, for a more comprehensive evaluation than our conference version.

**Prior SOTAs.** We compare with existing state-of-the-art text-to-image customization methods includes both optimization-based and optimization-free: (1) *Finetune-based*: DreamBooth [3], CustomDiffusion [10], Dream-Matcher [17]; (2) *Encoder-based*: ELITE [19], BLIP-Diffusion [20], IP-Adapter [43], MoMA [87], SSR-Encoder [88], Kosmos-G [86], Emu-2 [89], λ-ECLIPSE [90], MS-Diffusion [91]. Among these methods, Kosmos-G [86] and Emu-2 [89] are based on the multi-modal large language models.

Moreover, considering that there are also many methods focusing exclusively on human ID customized generation (a specific limited domain), we compare our approach with these methods in the human ID scenario to demonstrate our generalization, even though it is not the primary focus of this paper. We consider three recent state-of-the-art methods: PhotoMaker [23], Instant-ID [24], and PuLID [25].

## 4.2 Comparison with Stat-of-the-Arts

**Quantitative main results.** As shown in Table 1, RealCustom++ outperforms existing methods across all metrics on both SD-v1.5 and SDXL: (1) For text controllability, on the more powerful base model SDXL, we achieve relative improvements of 7.01%, 7.48%, and 76.43% on CLIP-B-T, CLIP-L-T, and ImageReward, respectively. The significant improvement on ImageReward validates RealCustom++’s core motivation: non-conflict real-word subject representation and disentangling the influence scope between given

Methods	CLIP-B-T(%)	CLIP-B-I(%)	DINO-I(%)
CustomDiffusion [10]	27.24	80.23	63.78
λ-ECLIPSE [90]	28.05	76.32	59.23
SSR-Encoder [88]	28.43	79.25	62.08
MS-Diffusion [91]	<u>30.02</u>	78.25	61.28
<b>RealCustom++(ours)</b>	<b>31.4</b>	<b>85.32</b>	<b>66.29</b>

TABLE 2: Quantitative comparisons on multiple-subject customization. RealCustom++ achieves state-of-the-art performance: for text controllability, we achieve a 4.6% improvement on CLIP-B-T; for subject similarity, we achieve 6.34% and 3.9% improvements on CLIP-B-I and DINO-I, respectively.

texts and subjects. This approach generates customized images with much higher quality, as other subject-irrelevant regions are completely controlled by the given text without contamination from the subjects. (2) For subject similarity, we achieve state-of-the-art performance on CLIP-B-I, CLIP-L-I, and DINO-I, validating that RealCustom++ can generate more similar subjects in the subject-relevant regions. The figure of “text-controllability (CLIP-B-T) versus subject-similarity (CLIP-B-I)” on SD-v1.5 in Figure 1(c) shows that the existing paradigm is trapped in the dual-optimum paradox, while RealCustom++ effectively eradicates it.

**Qualitative main results.** As shown in Figure 9, RealCustom++ demonstrates superior zero-shot open-domain customization capability for a wide range of subjects, including humans, characters, buildings, animals, and uniquely shaped toys. It generates higher-quality custom images with better subject similarity and text controllability compared to existing methods. Furthermore, the disentangled influence scope between subjects and texts allows RealCustom++ to produce cleaner and more diverse backgrounds. For instance, in the second row, existing methods like Custom-Diffusion and MS-Diffusion inherit the pink background from the given subject image, while RealCustom++ generates a background that aligns more closely with the prompt “on the beach”.

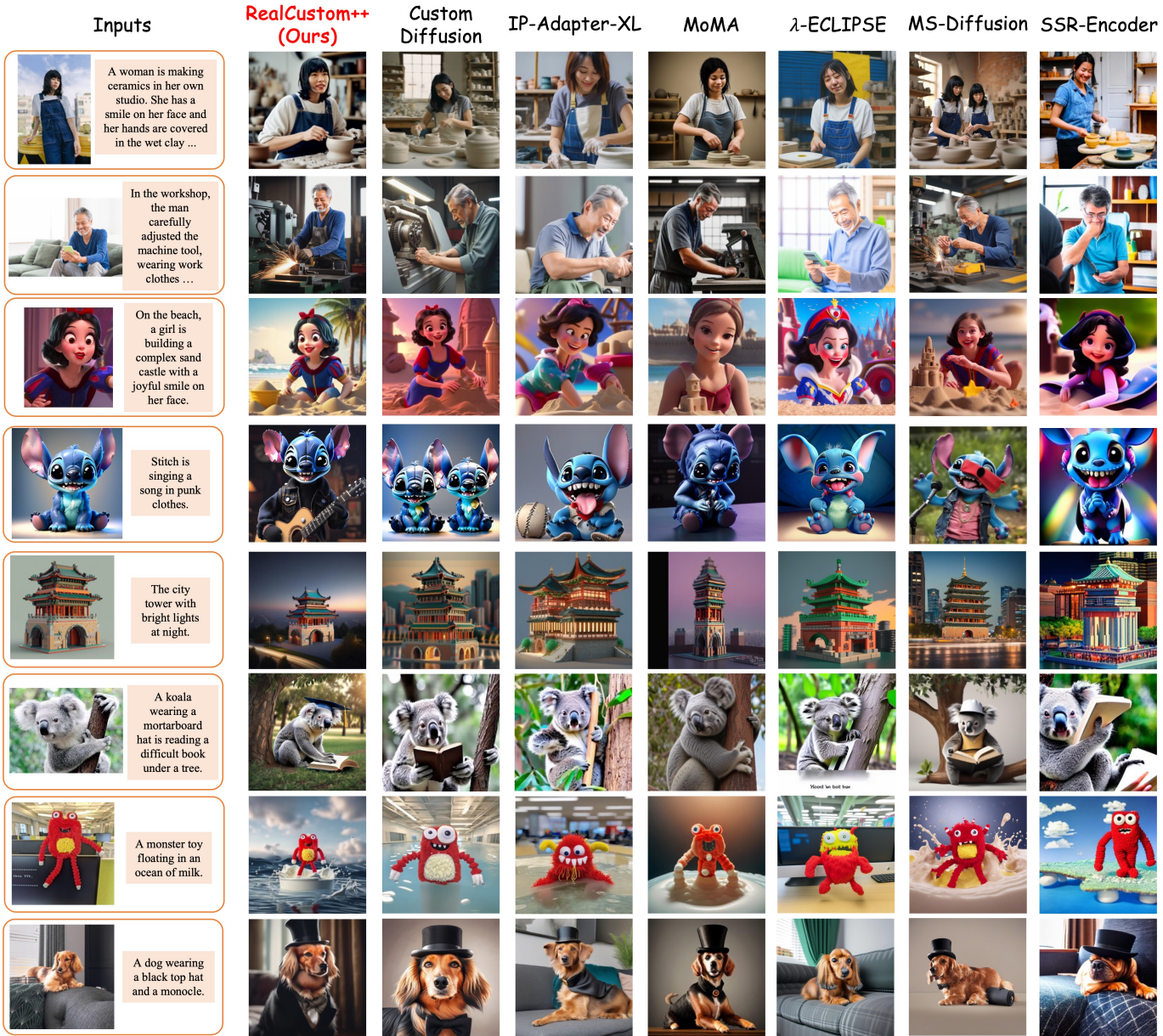


Fig. 9: Qualitative comparison with existing state-of-the-art customization methods. RealCustom++ produces higher quality results with better subject similarity and text controllability compared to existing methods. Additionally, RealCustom++ demonstrates superior subject diversity in poses and expressions (e.g., “smile on her face” in the first row). Furthermore, RealCustom++ generates customization results with cleaner and more diverse backgrounds. For instance, in the second row, existing methods like Custom-Diffusion and MS-Diffusion inherit the pink background from the given subject image, while RealCustom++ generates a background that aligns more closely with the prompt “on the beach.”

TopK ratio	CLIP-B-T $\uparrow$	CLIP-B-I $\uparrow$
$\gamma_{\text{scope}} = 0.1$	33.43	84.43
$\gamma_{\text{scope}} = 0.15$	33.43	86.09
$\gamma_{\text{scope}} = 0.2$	<b>33.43</b>	<b>87.32</b>
$\gamma_{\text{scope}} = 0.2$ w/o mask norm	30.26	87.32
$\gamma_{\text{scope}} = 0.3$	33.29	87.32
$\gamma_{\text{scope}} = 0.4$	32.62	87.32
$\gamma_{\text{scope}} = 0.5$	31.08	87.32

TABLE 3: Ablation study of using different Top-K  $\gamma_{\text{scope}}$  ratios.

**Comparison on multiple subjects customization.** To further evaluate the multiple-subject customization ability, following the common practice of previous works [12], [91],

we collect diverse subjects from previous works spanning various categories, including animals, characters, buildings, objects, etc., for a total of 30 different multiple subjects customized cases. The fully customized subjects and their prompts are provided in the Appendix. The subject similarity of multiple subjects is defined as the mean of each subject’s similarity. As illustrated in Table 2, we outperform existing state-of-the-art works in multiple-subject customization: for text controllability, we achieve a 4.6% improvement on CLIP-B-T; for subject similarity, we achieve 6.34% and 3.9% improvements on CLIP-B-I and DINO-I, respectively. The qualitative comparison shown in Figure 10 demonstrates that RealCustom++ generates multiple-

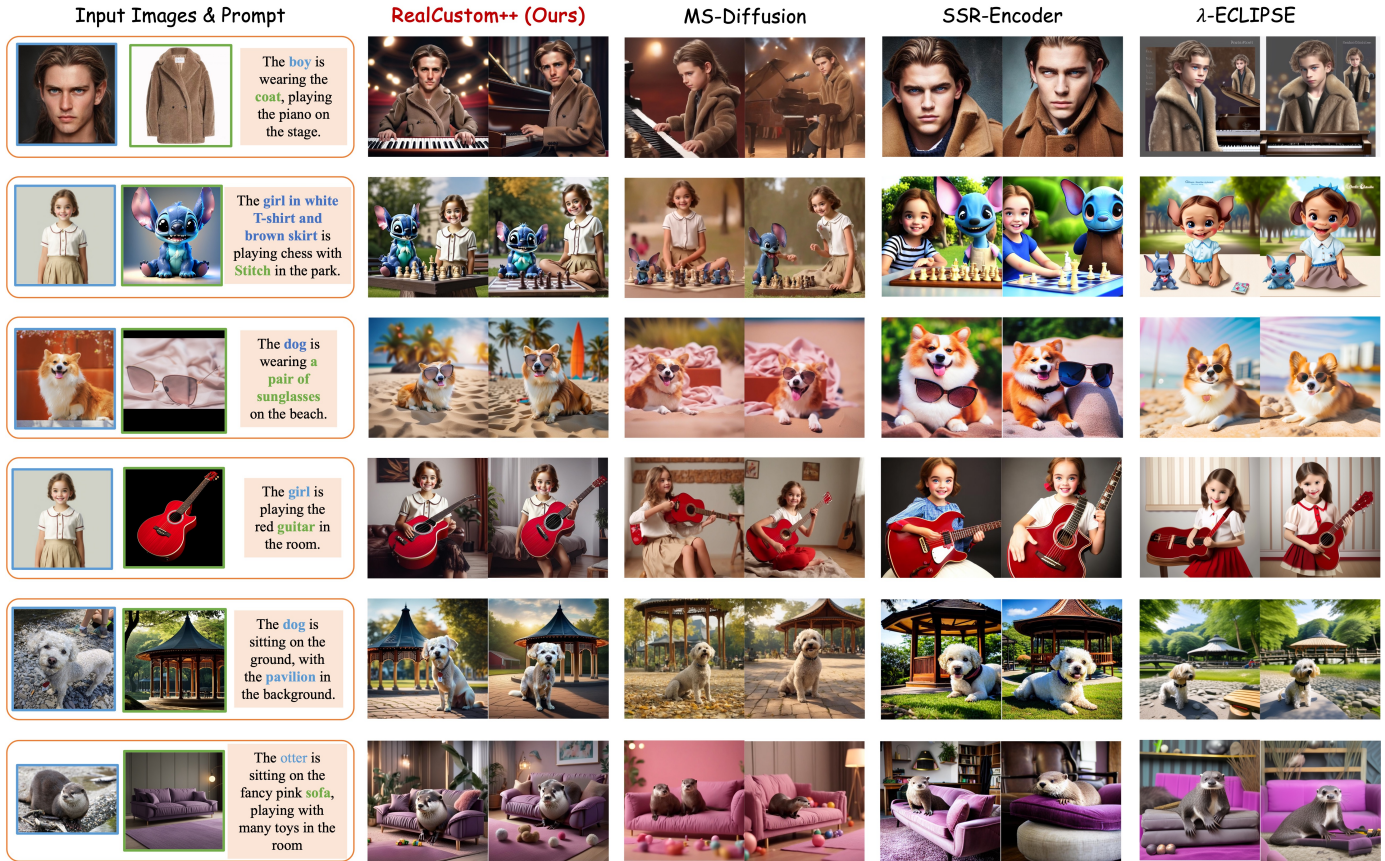


Fig. 10: Qualitative comparison for multiple-subject customization. We demonstrate that RealCustom++ generates multiple-subject customization results with superior text controllability and subject similarity compared to existing methods. For example, in the second row, RealCustom++ successfully generates the scene of the given “girl” playing chess with the given “Stitch”, while existing methods struggle to maintain consistency for both subjects. Moreover, RealCustom++ effectively handles diverse and complex interactions between different subjects, such as “wearing” in the first row and “playing guitar” in the fourth row.

No.	Attention Setting	CLIP-B-T $\uparrow$	CLIP-B-I $\uparrow$
(1)	all resolution cross-attn	32.06	83.97
(2)	low resolution cross-attn	32.20	84.23
(3)	(2) + all resolution self-attn	31.08	85.22
(4)	(2) + high resolution self-attn (Full Model)	<b>33.43</b>	<b>87.32</b>

TABLE 4: Ablation study on using different attentions to construct image mask guidance. The combination of low-resolution cross-attention and high-resolution self-attention provides the most accurate image mask for customization.

subject customization results with better text controllability and subject similarity than existing methods, aligning with the quantitative results in Table 2. For example, in the second row, RealCustom++ successfully generates the scene of the given “girl” playing chess with the given “Stitch,” while existing methods struggle to keep both subjects consistent. Moreover, RealCustom++ handles diverse and complex interactions between different subjects, such as “wearing” in the first row and “playing guitar” in the fourth row. Both the quantitative and qualitative results further validate the superiority of our proposed new paradigm, RealCustom++.

**Comparison on human ID customization.** Considering many existing customization methods focus solely on hu-

Early Stop Step	CLIP-B-T $\uparrow$	CLIP-B-I $\uparrow$
5	32.06	85.13
10	33.20	87.21
12	<b>33.43</b>	<b>87.32</b>
15	33.40	87.07
20	33.41	86.84
None (w/o early stop regularization)	33.41	86.67

TABLE 5: Ablation study of mask calculation early stop regularization for more temporally stable image mask guidance.

man ID customization [24], [25], [26], [42] (a specific limited domain), we further provide a qualitative comparison with these methods in Figure 11, demonstrating that our open-domain paradigm, RealCustom++, can also effectively generalize to this specific domain, even though human ID customization is not the primary focus of this paper. Specifically, RealCustom++ generates consistent IDs (as shown in the first two rows) while preserving elements such as clothing, hairstyles, and accessories (illustrated in the last three rows), which is challenging for existing methods.

### 4.3 Ablations

We ablate each component of our proposed RealCustom++ on SDXL, which mainly includes: (1) the adaptive mask guidance for disentangling the influence scope between the

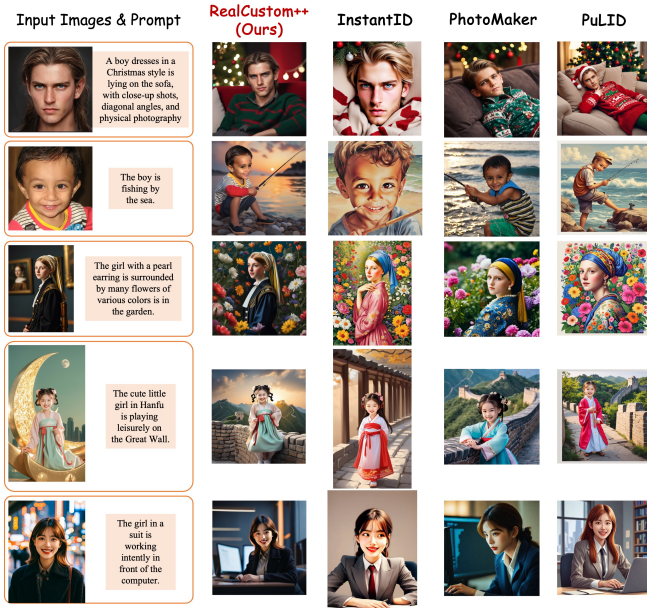


Fig. 11: Qualitative comparison with existing ID customization methods. We demonstrate that our proposed open-domain paradigm, RealCustom++, effectively generalizes to the human ID domain. Specifically, RealCustom++ generates consistent IDs (as shown in the first two rows) while preserving elements such as clothing, hairstyles, and accessories (illustrated in the last three rows), which is challenging for existing methods.

text and the subjects; (2) the cross-layer cross-scale projector for effectively encoding the subject image features; and (3) the curriculum training recipe for effective training.

**Effectiveness of adaptive mask guidance.** We first visualize the real-word customization process in single-subject customization in Figure 12 and multiple-subject customization in Figure 13. In Figure 12, we show that the attention map of the target real words gradually forms into the given subjects with details added step by step, achieving open-domain zero-shot customization while keeping other subject-irrelevant parts completely controlled by the given text. Moreover, we show that RealCustom++ can adapt to shape variation (e.g., the second row in Figure 12) and subject overlaps (e.g., the third row in Figure 12). In the multiple-subject customization visualization in Figure 13, we show that RealCustom++ provides accurate and decoupled guidance masks for each given subject, thereby achieving high-quality similarity for each subject.

We then ablate the choice of using different attention to construct a more spatially accurate image mask guidance. As shown in Table 4, the combination of low-resolution cross-attention and high-resolution self-attention provides the most accurate image mask for customization, resulting in the best text controllability and subject similarity. We also visualize their differences in Figure 14, showing that (1) solely relying on cross-attention maps results in scattered mask guidance (e.g., the image guidance mask for the backpack, where holes exist in the center of the mask), causing the degradation of subject details; (2) using all-resolution self-attention maps makes the guidance mask over-focused, resulting in the degradation of mask accuracy.

The ablation study of early stop regularization for more

No.	Projector Setting	CLIP-B-T $\uparrow$	CLIP-B-I $\uparrow$
(1)	MLP(naive projector)	33.21	83.32
(2)	(1)+cross-layer mechanism	33.45	86.12
(3)	(2)+cross-scale mechanism (Full Model)	33.43	87.32

TABLE 6: Ablation study of the cross-layer cross-scale projector.

Feature Combination Setting	CLIP-B-T $\uparrow$	CLIP-B-I $\uparrow$
cross-scale element add	29.94	86.33
+ cross-layer token concat		
cross-scale token concat	33.65	85.62
+ cross-layer token concat		
cross-scale token concat	33.43	87.32
+ cross-layer element add (Final Model)		

TABLE 7: Ablation study of different feature combination.

temporally stable image mask guidance is provided in Table 5. This aligns with our motivation shown in Figure 8, where the image guidance mask tends to converge in the middle diffusion steps, and reusing the middle step’s mask increases both similarity and controllability.

The qualitative and quantitative results of using different Top-K ratios  $\gamma_{\text{scope}}$  are shown in Table 3 and Figure 15, respectively. We conclude that: (1) Within a proper range (experimentally,  $\gamma_{\text{scope}} \in [0.15, 0.4]$ ), the results are quite robust. (2) The maximum normalization in Eq. 15 is important for achieving both high similarity and controllability, as different regions in the selected parts have varying subject relevance and should be assigned different weights. (3) Too small or too large an influence scope will degrade similarity or controllability, respectively.

Finally, we ablate the impact of using different real words for customization in Figure 16. The customized real word is highlighted in red. We show that: (1) In the first row, regardless of how coarse-grained the word is, the customization results of RealCustom++ are quite robust. (2) In the second row, using completely different words to represent the given subject opens a door for a new application: novel concept creation. RealCustom++ combines these two concepts to create a new one, e.g., generating a tiger with the appearance of the given white Bichon Frise, as shown in the second row of Figure 16.

**Effectiveness of cross-layer cross-scale projector.** As shown in Table 6, we ablate the design of our proposed cross-layer cross-scale projector, showing that both the cross-layer enhancement and the cross-scale enhancement bring substantial improvement over subject-similarity while cost little text-controllability, which validates our key idea of encoding subject images, i.e., keeping deep features’ “dominating” position to avoid compromising their effectiveness of initial good alignment with the text condition

We next ablate the choice of different feature combinations in Table 7. The results validate our hypothesis that same-level features should be added element-wise, while different-level features should be concatenated token-wise to avoid conflicts.

**Effectiveness of curriculum training recipe.** As shown in Table 8, we conclude that: (1) Training the model solely on `<text-image>` or `<multiview>` data significantly decreases either text controllability or subject similarity. This

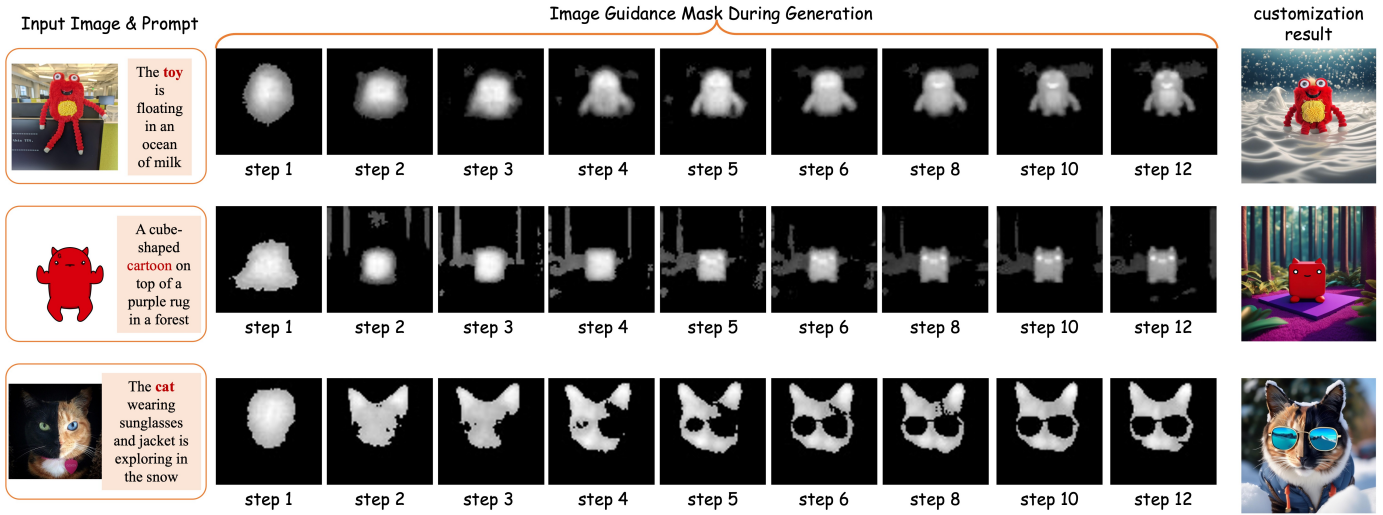


Fig. 12: Illustration of gradually customizing the target real words into the given subjects for single-subject customization. The customized words are highlighted in red, with their attention maps gradually forming into the given subjects and details being added step by step. This process provides a more accurate image guidance mask for open-domain customization, while the remaining subject-irrelevant parts are completely controlled by the given text.

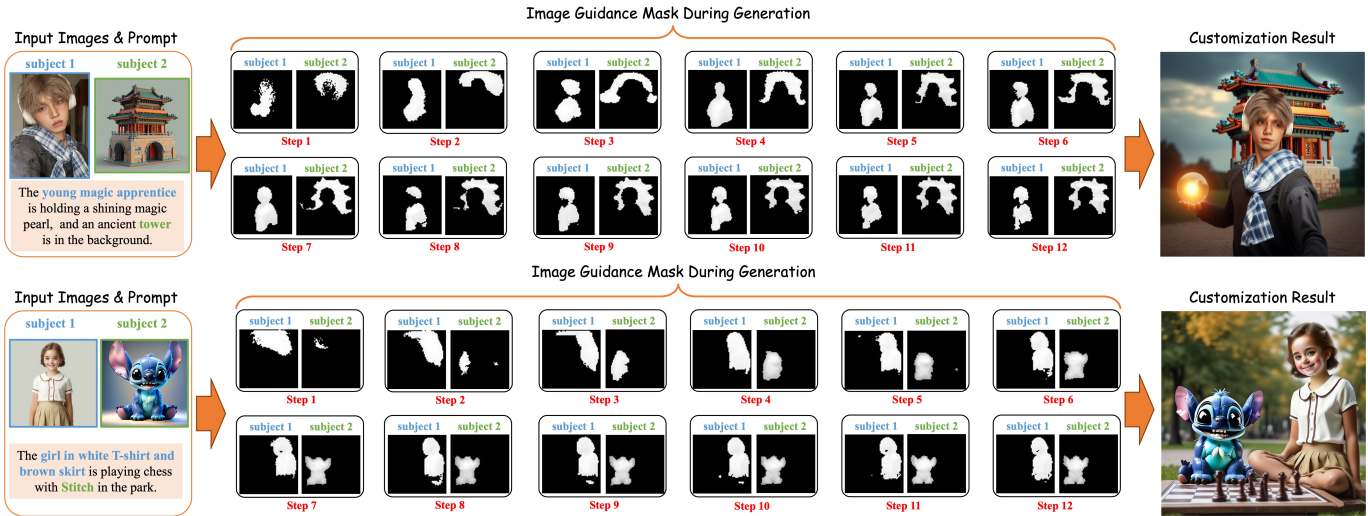


Fig. 13: Illustration of gradually customizing the native real words into the given subjects for multiple-subject customization. The different customized words in each case are highlighted in blue and green, respectively. We show that RealCustom++ provides accurate and decoupled guidance masks for each given subject, thereby achieving high-quality similarity for each subject.

No.	Training Recipe	CLIP-B-T $\uparrow$	CLIP-B-I $\uparrow$
(1)	<text-image> data only	30.02	86.24
(2)	<multiview> data only	32.18	83.92
(3)	<text-image> data + $p_{\text{text-image}} = p_{\text{multiview}} = 0.5$	31.89	85.33
(4)	<text-image> data + <multiview> data + curriculum data strategy	32.10	86.11
(5)	(4) + cropping strategy with a fixed random ratio between $[1, \sqrt{10}]$	33.43	86.82
(6)	(4) + curriculum cropping strategy (Full Model)	33.43	87.32

TABLE 8: Ablation study of the curriculum training recipe.

is because <text-image> data lacks subject pose diversity, while <multiview> data lacks open-domain subject diversity. (2) The curriculum data strategy achieves better CLIP-B-T and CLIP-B-I scores compared to naively using a 50% probability of <text-image> or <multiview> data. (3) The proposed curriculum cropping strategy further improves both metrics, highlighting the importance of promoting more stable initial convergence and better subsequent size generalization.

## 5 DISCUSSION

Despite the superior real-time open-domain customization achieved, RealCustom++ still has several limitations: (1) The inference paradigm of RealCustom++ includes a guidance branch and a generation branch, requiring the diffusion



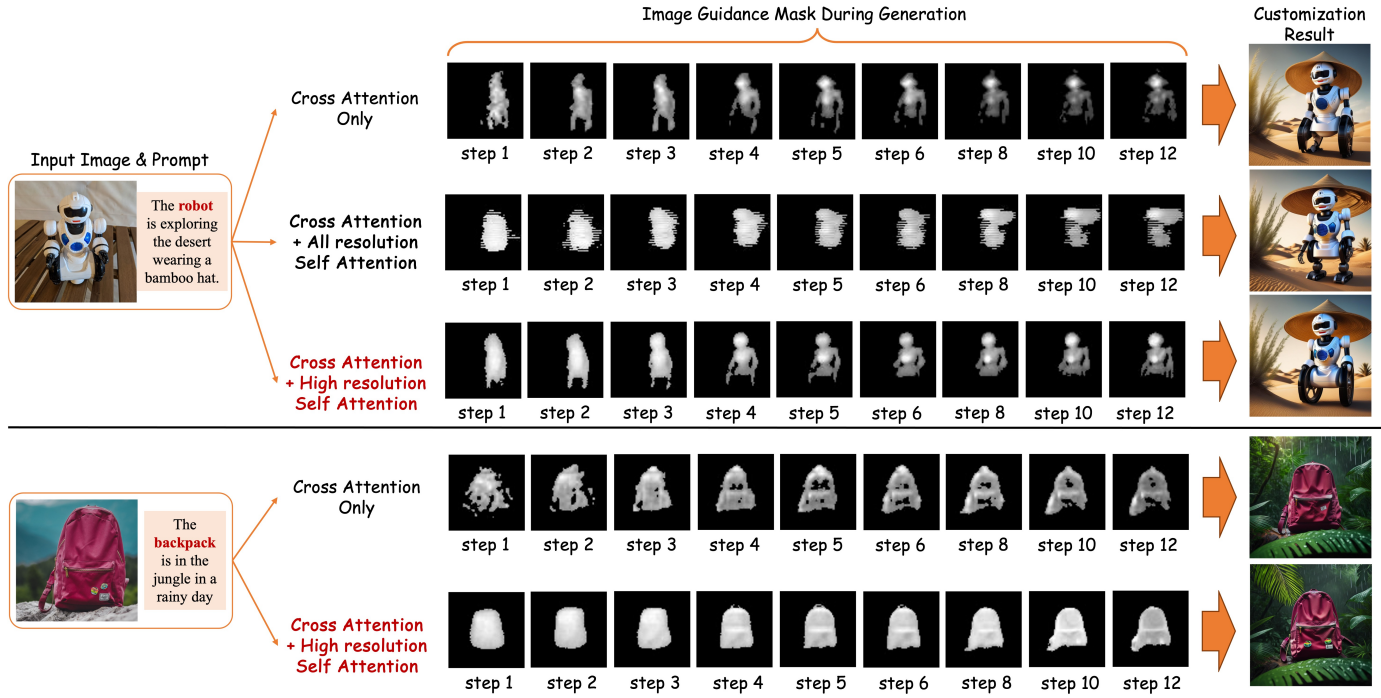


Fig. 14: Visualization of using different attention mask to construct image guidance mask. We show that (1) solely relying on cross attention map results in scattered mask guidance results in the degradation of subject details; (2) using all resolution self-attention map will make the guidance mask over-focused, resulting in the degradation of mask accuracy.

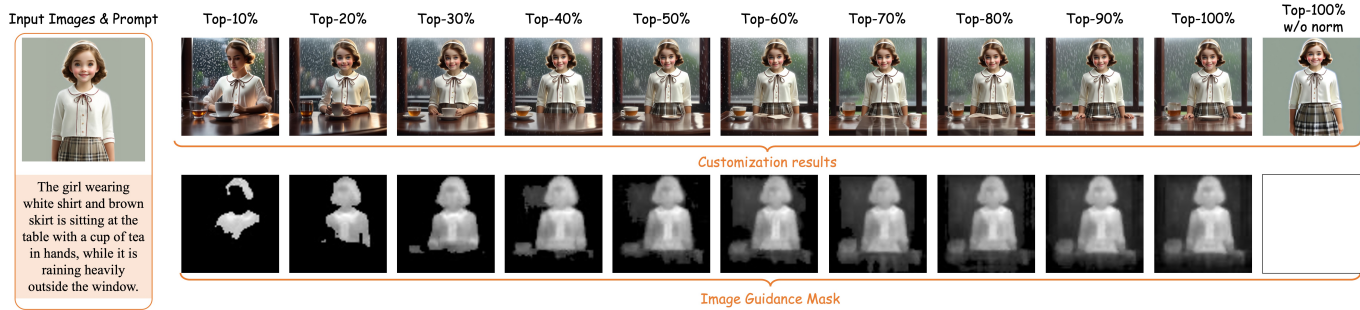


Fig. 15: Visualization of different influence scope.

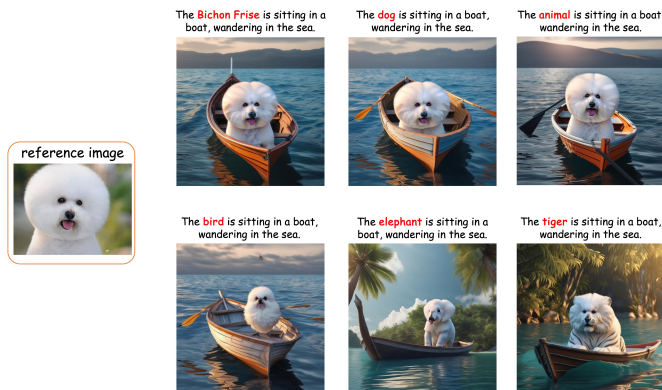


Fig. 16: Customization using different native real words. The customized words are highlighted in red.

is nearly twice that of standard text-to-image generation. Although our proposed mask calculation early stop regularization can reuse the previous steps' mask, requiring only a single generation branch in the later steps, the time cost is still almost 1.5 times that of standard text-to-image generation. (2) The key idea of RealCustom++ is to gradually customize the generation of the target real words into the given subjects while leaving other subject-irrelevant regions completely controlled by the given text. Therefore, RealCustom++ relies on the generation ability of the pre-trained text-to-image diffusion models. If the pre-trained text-to-image models cannot generate the concept of the target real word, RealCustom++ cannot customize the specific subject generation of this target word. In other words, the failure cases of RealCustom++ lie in the failure cases of the pre-trained text-to-image diffusion models themselves. As shown in Figure 17, when SDXL fails to generate an image aligned with the given text (e.g., SDXL fails to generate a woman), RealCustom++ usually also fails to customize the

Unet to be forwarded twice in each step. As a result, the text-to-image customized generation time cost by RealCustom++

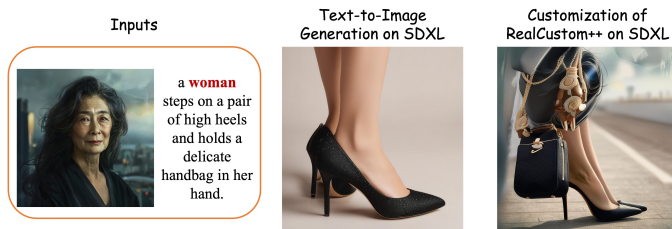


Fig. 17: The failure cases of RealCustom++ are primarily due to the limitations of the pre-trained text-to-image diffusion models. When SDXL fails to generate an image aligned with the given text, RealCustom++ typically also fails.

generation of “woman” into the given one. The stronger the pre-trained text-to-image diffusion models, the better the customization ability of RealCustom++.

## 6 CONCLUSION

In this paper, we present a novel customization paradigm, RealCustom++, that, for the first time, represents given subjects as non-conflict real words, thereby disentangling the similarity of given subjects from the controllability of given text by precisely limiting subject influence to relevant parts. This is achieved by gradually customizing the target real word from its general concept to the specific subject within a novel “train-inference” decoupled framework. Specifically, during training, RealCustom++ learns the general alignment capabilities between visual conditions and all the words in the pre-trained models’ original text conditions. This is achieved through a novel cross-layer cross-scale projector to robustly and finely extract subject features, and a novel curriculum training recipe to adapt the generated subject to diverse poses and sizes. During inference, based on the learned alignment, RealCustom++ customizes the generation of the target real words while keeping other subject-irrelevant regions uncontaminated through a novel adaptive mask guidance. Moreover, we propose a novel multi-real-words customization algorithm to extend RealCustom++ to accommodate multiple-subject customization across various tasks. Extensive experiments demonstrate that RealCustom++ achieves the unity of high-quality similarity and controllability in real-time open-domain scenarios for both single-subject and multiple-subject customization.

## ACKNOWLEDGMENTS

We would like to thank our colleagues at ByteDance, Yiming Luo, for his valuable help with multi-view data processing. We also thank Wei Liu and Shiqi Sun for their valuable discussions at the very beginning of this research.

## REFERENCES

[1] F.-A. Croitoru, V. Hondru, R. T. Ionescu, and M. Shah, “Diffusion models in vision: A survey,” *IEEE Transactions on Pattern Analysis and Machine Intelligence*, vol. 45, no. 9, pp. 10 850–10 869, 2023.

[2] R. Gal, Y. Alaluf, Y. Atzmon, O. Patashnik, A. H. Bermano, G. Chechik, and D. Cohen-Or, “An image is worth one word: Personalizing text-to-image generation using textual inversion,” *arXiv preprint arXiv:2208.01618*, 2022.

[3] N. Ruiz, Y. Li, V. Jampani, Y. Pritch, M. Rubinstein, and K. Aberman, “Dreambooth: Fine tuning text-to-image diffusion models for subject-driven generation,” in *Proceedings of the IEEE/CVF Conference on Computer Vision and Pattern Recognition*, 2023, pp. 22 500–22 510.

[4] A. Ramesh, M. Pavlov, G. Goh, S. Gray, C. Voss, A. Radford, M. Chen, and I. Sutskever, “Zero-shot text-to-image generation,” in *International conference on machine learning*. Pmlr, 2021, pp. 8821–8831.

[5] H. Zhang, T. Xu, H. Li, S. Zhang, X. Wang, X. Huang, and D. N. Metaxas, “Stackgan++: Realistic image synthesis with stacked generative adversarial networks,” *IEEE transactions on pattern analysis and machine intelligence*, vol. 41, no. 8, pp. 1947–1962, 2018.

[6] J. Sun, Q. Deng, Q. Li, M. Sun, Y. Liu, and Z. Sun, “Anyface++: A unified framework for free-style text-to-face synthesis and manipulation,” *IEEE Transactions on Pattern Analysis and Machine Intelligence*, 2024.

[7] T. Hinz, S. Heinrich, and S. Wermter, “Semantic object accuracy for generative text-to-image synthesis,” *IEEE transactions on pattern analysis and machine intelligence*, vol. 44, no. 3, pp. 1552–1565, 2020.

[8] R. Rombach, A. Blattmann, D. Lorenz, P. Esser, and B. Ommer, “High-resolution image synthesis with latent diffusion models,” in *Proceedings of the IEEE/CVF conference on computer vision and pattern recognition*, 2022, pp. 10 684–10 695.

[9] D. Podell, Z. English, K. Lacey, A. Blattmann, T. Dockhorn, J. Müller, J. Penna, and R. Rombach, “Sdxl: Improving latent diffusion models for high-resolution image synthesis,” *arXiv preprint arXiv:2307.01952*, 2023.

[10] N. Kumari, B. Zhang, R. Zhang, E. Shechtman, and J.-Y. Zhu, “Multi-concept customization of text-to-image diffusion,” in *Proceedings of the IEEE/CVF Conference on Computer Vision and Pattern Recognition*, 2023, pp. 1931–1941.

[11] L. Han, Y. Li, H. Zhang, P. Milanfar, D. Metaxas, and F. Yang, “Svdiff: Compact parameter space for diffusion fine-tuning,” in *Proceedings of the IEEE/CVF International Conference on Computer Vision*, 2023, pp. 7323–7334.

[12] Z. Liu, Y. Zhang, Y. Shen, K. Zheng, K. Zhu, R. Feng, Y. Liu, D. Zhao, J. Zhou, and Y. Cao, “Cones 2: Customizable image synthesis with multiple subjects,” *arXiv preprint arXiv:2305.19327*, 2023.

[13] Y. Alaluf, E. Richardson, G. Metzger, and D. Cohen-Or, “A neural space-time representation for text-to-image personalization,” *arXiv preprint arXiv:2305.15391*, 2023.

[14] Y. Zhang, W. Dong, F. Tang, N. Huang, H. Huang, C. Ma, T.-Y. Lee, O. Deussen, and C. Xu, “Prospect: Expanded conditioning for the personalization of attribute-aware image generation,” *arXiv preprint arXiv:2305.16225*, 2023.

[15] A. Voynov, Q. Chu, D. Cohen-Or, and K. Aberman, “p+: Extended textual conditioning in text-to-image generation,” *arXiv preprint arXiv:2303.09522*, 2023.

[16] G. Daras and A. G. Dimakis, “Multiresolution textual inversion,” *arXiv preprint arXiv:2211.17115*, 2022.

[17] J. Nam, H. Kim, D. Lee, S. Jin, S. Kim, and S. Chang, “Dream-matcher: Appearance matching self-attention for semantically-consistent text-to-image personalization,” in *Proceedings of the IEEE/CVF Conference on Computer Vision and Pattern Recognition*, 2024, pp. 8100–8110.

[18] M. Hua, J. Liu, F. Ding, W. Liu, J. Wu, and Q. He, “Dream-tuner: Single image is enough for subject-driven generation,” *arXiv preprint arXiv:2312.13691*, 2023.

[19] Y. Wei, Y. Zhang, Z. Ji, J. Bai, L. Zhang, and W. Zuo, “Elite: Encoding visual concepts into textual embeddings for customized text-to-image generation,” in *Proceedings of the IEEE/CVF International Conference on Computer Vision*, 2023, pp. 15 943–15 953.

[20] D. Li, J. Li, and S. Hoi, “Blip-diffusion: Pre-trained subject representation for controllable text-to-image generation and editing,” *Advances in Neural Information Processing Systems*, vol. 36, 2024.

[21] J. Shi, W. Xiong, Z. Lin, and H. J. Jung, “Instantbooth: Personalized text-to-image generation without test-time finetuning,” *arXiv preprint arXiv:2304.03411*, 2023.

[22] R. Gal, M. Arar, Y. Atzmon, A. H. Bermano, G. Chechik, and D. Cohen-Or, “Designing an encoder for fast personalization of text-to-image models,” *arXiv preprint arXiv:2302.12228*, 2023.

[23] Z. Li, M. Cao, X. Wang, Z. Qi, M.-M. Cheng, and Y. Shan, “Photomaker: Customizing realistic human photos via stacked id embedding,” in *Proceedings of the IEEE/CVF Conference on Computer Vision and Pattern Recognition*, 2024, pp. 8640–8650.

- [24] Q. Wang, X. Bai, H. Wang, Z. Qin, and A. Chen, "Instantid: Zero-shot identity-preserving generation in seconds," *arXiv preprint arXiv:2401.07519*, 2024.
- [25] Z. Guo, Y. Wu, Z. Chen, L. Chen, and Q. He, "Pulid: Pure and lightning id customization via contrastive alignment," *arXiv preprint arXiv:2404.16022*, 2024.
- [26] G. Xiao, T. Yin, W. T. Freeman, F. Durand, and S. Han, "Fastcomposer: Tuning-free multi-subject image generation with localized attention," *arXiv preprint arXiv:2305.10431*, 2023.
- [27] Z. Chen, S. Fang, W. Liu, Q. He, M. Huang, Y. Zhang, and Z. Mao, "Dreamidentity: Improved editability for efficient face-identity preserved image generation," *arXiv preprint arXiv:2307.00300*, 2023.
- [28] C. Raffel, N. Shazeer, A. Roberts, K. Lee, S. Narang, M. Matena, Y. Zhou, W. Li, and P. J. Liu, "Exploring the limits of transfer learning with a unified text-to-text transformer," *Journal of machine learning research*, vol. 21, no. 140, pp. 1–67, 2020.
- [29] A. Radford, J. W. Kim, C. Hallacy, A. Ramesh, G. Goh, S. Agarwal, G. Sastry, A. Askell, P. Mishkin, J. Clark *et al.*, "Learning transferable visual models from natural language supervision," in *International conference on machine learning*. PMLR, 2021, pp. 8748–8763.
- [30] A. Kuznetsova, H. Rom, N. Alldrin, J. Uijlings, I. Krasin, J. Pont-Tuset, S. Kamali, S. Popov, M. Mallocci, A. Kolesnikov *et al.*, "The open images dataset v4: Unified image classification, object detection, and visual relationship detection at scale," *International Journal of Computer Vision*, vol. 128, no. 7, pp. 1956–1981, 2020.
- [31] M. Huang, Z. Mao, M. Liu, Q. He, and Y. Zhang, "Realcustom: Narrowing real text word for real-time open-domain text-to-image customization," in *Proceedings of the IEEE/CVF Conference on Computer Vision and Pattern Recognition*, 2024, pp. 7476–7485.
- [32] M. Huang, Z. Mao, P. Wang, Q. Wang, and Y. Zhang, "Dse-gan: Dynamic semantic evolution generative adversarial network for text-to-image generation," in *Proceedings of the 30th ACM International Conference on Multimedia*, 2022, pp. 4345–4354.
- [33] C. Saharia, J. Ho, W. Chan, T. Salimans, D. J. Fleet, and M. Norouzi, "Image super-resolution via iterative refinement," *IEEE transactions on pattern analysis and machine intelligence*, vol. 45, no. 4, pp. 4713–4726, 2022.
- [34] M. Zhang, Z. Cai, L. Pan, F. Hong, X. Guo, L. Yang, and Z. Liu, "Motiondiffuse: Text-driven human motion generation with diffusion model," *IEEE Transactions on Pattern Analysis and Machine Intelligence*, 2024.
- [35] Y. Luo, Q. Yang, Y. Fan, H. Qi, and M. Xia, "Measurement guidance in diffusion models: Insight from medical image synthesis," *IEEE Transactions on Pattern Analysis and Machine Intelligence*, 2024.
- [36] M. Li, J. Lin, C. Meng, S. Ermon, S. Han, and J.-Y. Zhu, "Efficient spatially sparse inference for conditional gans and diffusion models," *IEEE Transactions on Pattern Analysis and Machine Intelligence*, 2023.
- [37] Z. Dong, P. Wei, and L. Lin, "Dreamartist: Towards controllable one-shot text-to-image generation via contrastive prompt-tuning," *arXiv preprint arXiv:2211.11337*, 2022.
- [38] X. Jia, Y. Zhao, K. C. Chan, Y. Li, H. Zhang, B. Gong, T. Hou, H. Wang, and Y.-C. Su, "Taming encoder for zero fine-tuning image customization with text-to-image diffusion models," *arXiv preprint arXiv:2304.02642*, 2023.
- [39] S. Hao, K. Han, S. Zhao, and K.-Y. K. Wong, "Vico: Detail-preserving visual condition for personalized text-to-image generation," *arXiv preprint arXiv:2306.00971*, 2023.
- [40] T. Karras, S. Laine, and T. Aila, "A style-based generator architecture for generative adversarial networks," in *Proceedings of the IEEE/CVF conference on computer vision and pattern recognition*, 2019, pp. 4401–4410.
- [41] J. Ma, J. Liang, C. Chen, and H. Lu, "Subject-diffusion: Open domain personalized text-to-image generation without test-time fine-tuning," *arXiv preprint arXiv:2307.11410*, 2023.
- [42] Z. Li, M. Cao, X. Wang, Z. Qi, M.-M. Cheng, and Y. Shan, "Photomaker: Customizing realistic human photos via stacked id embedding," *arXiv preprint arXiv:2312.04461*, 2023.
- [43] H. Ye, J. Zhang, S. Liu, X. Han, and W. Yang, "Ip-adapter: Text compatible image prompt adapter for text-to-image diffusion models," *arXiv preprint arXiv:2308.06721*, 2023.
- [44] O. Avrahami, K. Aberman, O. Fried, D. Cohen-Or, and D. Lischinski, "Break-a-scene: Extracting multiple concepts from a single image," in *SIGGRAPH Asia 2023 Conference Papers*, 2023, pp. 1–12.
- [45] C. Jin, R. Tanno, A. Saseendran, T. Diethe, and P. Teare, "An image is worth multiple words: Learning object level concepts using multi-concept prompt learning," *arXiv preprint arXiv:2310.12274*, 2023.
- [46] N. Otsu *et al.*, "A threshold selection method from gray-level histograms," *Automatica*, vol. 11, no. 285–296, pp. 23–27, 1975.
- [47] Y. Zhang, M. Yang, Q. Zhou, and Z. Wang, "Attention calibration for disentangled text-to-image personalization," *arXiv preprint arXiv:2403.18551*, 2024.
- [48] Y. Gu, X. Wang, J. Z. Wu, Y. Shi, Y. Chen, Z. Fan, W. Xiao, R. Zhao, S. Chang, W. Wu *et al.*, "Mix-of-show: Decentralized low-rank adaptation for multi-concept customization of diffusion models," *Advances in Neural Information Processing Systems*, vol. 36, 2024.
- [49] E. J. Hu, Y. Shen, P. Wallis, Z. Allen-Zhu, Y. Li, S. Wang, L. Wang, and W. Chen, "Lora: Low-rank adaptation of large language models," *arXiv preprint arXiv:2106.09685*, 2021.
- [50] C. Zhu, K. Li, Y. Ma, C. He, and L. Xiu, "Multiboost: Towards generating all your concepts in an image from text," *arXiv preprint arXiv:2404.14239*, 2024.
- [51] A. Ramesh, P. Dhariwal, A. Nichol, C. Chu, and M. Chen, "Hierarchical text-conditional image generation with clip latents," *arXiv preprint arXiv:2204.06125*, vol. 1, no. 2, p. 3, 2022.
- [52] C. Saharia, W. Chan, S. Saxena, L. Li, J. Whang, E. L. Denton, K. Ghasemipour, R. Gontijo Lopes, B. Karagol Ayan, T. Salimans *et al.*, "Photorealistic text-to-image diffusion models with deep language understanding," *Advances in Neural Information Processing Systems*, vol. 35, pp. 36 479–36 494, 2022.
- [53] W. Chen, H. Hu, C. Saharia, and W. W. Cohen, "Re-imagen: Retrieval-augmented text-to-image generator," *arXiv preprint arXiv:2209.14491*, 2022.
- [54] Y. Balaji, S. Nah, X. Huang, A. Vahdat, J. Song, K. Kreis, M. Aittala, T. Aila, S. Laine, B. Catanzaro *et al.*, "ediffi: Text-to-image diffusion models with an ensemble of expert denoisers," *arXiv preprint arXiv:2211.01324*, 2022.
- [55] A. Hertz, R. Mokady, J. Tenenbaum, K. Aberman, Y. Pritch, and D. Cohen-Or, "Prompt-to-prompt image editing with cross attention control," *arXiv preprint arXiv:2208.01626*, 2022.
- [56] M. Cao, X. Wang, Z. Qi, Y. Shan, X. Qie, and Y. Zheng, "Masactrl: Tuning-free mutual self-attention control for consistent image synthesis and editing," *arXiv preprint arXiv:2304.08465*, 2023.
- [57] J. Song, C. Meng, and S. Ermon, "Denoising diffusion implicit models," *arXiv preprint arXiv:2010.02502*, 2020.
- [58] Y. Li, H. Liu, Q. Wu, F. Mu, J. Yang, J. Gao, C. Li, and Y. J. Lee, "Gligen: Open-set grounded text-to-image generation," in *Proceedings of the IEEE/CVF Conference on Computer Vision and Pattern Recognition*, 2023, pp. 22 511–22 521.
- [59] Z. Li, Q. Zhou, X. Zhang, Y. Zhang, Y. Wang, and W. Xie, "Guiding text-to-image diffusion model towards grounded generation," *arXiv preprint arXiv:2301.05221*, 2023.
- [60] H. Chefer, Y. Alaluf, Y. Vinker, L. Wolf, and D. Cohen-Or, "Attend-and-excite: Attention-based semantic guidance for text-to-image diffusion models," *ACM Transactions on Graphics (TOG)*, vol. 42, no. 4, pp. 1–10, 2023.
- [61] Y. Li, M. Keuper, D. Zhang, and A. Khoreva, "Divide & bind your attention for improved generative semantic nursing," *arXiv preprint arXiv:2307.10864*, 2023.
- [62] W. Wu, Y. Zhao, M. Z. Shou, H. Zhou, and C. Shen, "Dif-fumask: Synthesizing images with pixel-level annotations for semantic segmentation using diffusion models," *arXiv preprint arXiv:2303.11681*, 2023.
- [63] C. Xiao, Q. Yang, F. Zhou, and C. Zhang, "From text to mask: Localizing entities using the attention of text-to-image diffusion models," *arXiv preprint arXiv:2309.04109*, 2023.
- [64] J. Wang, X. Li, J. Zhang, Q. Xu, Q. Zhou, Q. Yu, L. Sheng, and D. Xu, "Diffusion model is secretly a training-free open vocabulary semantic segmenter," *arXiv preprint arXiv:2309.02773*, 2023.
- [65] Y. Bengio, J. Louradour, R. Collobert, and J. Weston, "Curriculum learning," in *Proceedings of the 26th annual international conference on machine learning*, 2009, pp. 41–48.
- [66] X. Wang, Y. Chen, and W. Zhu, "A survey on curriculum learning," *IEEE transactions on pattern analysis and machine intelligence*, vol. 44, no. 9, pp. 4555–4576, 2021.
- [67] Y. Wang, Y. Yue, R. Lu, Y. Han, S. Song, and G. Huang, "Efficient-train++: Generalized curriculum learning for efficient visual backbone training," *IEEE Transactions on Pattern Analysis and Machine Intelligence*, 2024.

- [68] S. Wu, T. Zhou, Y. Du, J. Yu, B. Han, and T. Liu, "A time-consistency curriculum for learning from instance-dependent noisy labels," *IEEE Transactions on Pattern Analysis and Machine Intelligence*, 2024.
- [69] E. A. Platanios, O. Stretcu, G. Neubig, B. Póczos, and T. M. Mitchell, "Competence-based curriculum learning for neural machine translation," *arXiv preprint arXiv:1903.09848*, 2019.
- [70] B. Xu, Q. Wang, Y. Lyu, Y. Zhu, and Z. Mao, "Entity structure within and throughout: Modeling mention dependencies for document-level relation extraction," in *Proceedings of the AAAI conference on artificial intelligence*, vol. 35, no. 16, 2021, pp. 14 149–14 157.
- [71] Y. Wei, X. Liang, Y. Chen, X. Shen, M.-M. Cheng, J. Feng, Y. Zhao, and S. Yan, "Stc: A simple to complex framework for weakly-supervised semantic segmentation," *IEEE transactions on pattern analysis and machine intelligence*, vol. 39, no. 11, pp. 2314–2320, 2016.
- [72] Y. Tsvetkov, M. Faruqui, W. Ling, B. MacWhinney, and C. Dyer, "Learning the curriculum with bayesian optimization for task-specific word representation learning," *arXiv preprint arXiv:1605.03852*, 2016.
- [73] P. Soviany, C. Ardei, R. T. Ionescu, and M. Leordeanu, "Image difficulty curriculum for generative adversarial networks (cugan)," in *Proceedings of the IEEE/CVF winter conference on applications of computer vision*, 2020, pp. 3463–3472.
- [74] R. Tudor Ionescu, B. Alexe, M. Leordeanu, M. Popescu, D. P. Papadopoulos, and V. Ferrari, "How hard can it be? estimating the difficulty of visual search in an image," in *Proceedings of the IEEE Conference on Computer Vision and Pattern Recognition*, 2016, pp. 2157–2166.
- [75] V. Cirik, E. Hovy, and L.-P. Morency, "Visualizing and understanding curriculum learning for long short-term memory networks," *arXiv preprint arXiv:1611.06204*, 2016.
- [76] T. Kocmi and O. Bojar, "Curriculum learning and mini-batch bucketing in neural machine translation," *arXiv preprint arXiv:1707.09533*, 2017.
- [77] C. Liu, S. He, K. Liu, J. Zhao *et al.*, "Curriculum learning for natural answer generation." in *IJCAI*, 2018, pp. 4223–4229.
- [78] T. Matisen, A. Oliver, T. Cohen, and J. Schulman, "Teacher-student curriculum learning," *IEEE transactions on neural networks and learning systems*, vol. 31, no. 9, pp. 3732–3740, 2019.
- [79] O. Ronneberger, P. Fischer, and T. Brox, "U-net: Convolutional networks for biomedical image segmentation," in *Medical Image Computing and Computer-Assisted Intervention–MICCAI 2015: 18th International Conference, Munich, Germany, October 5-9, 2015, Proceedings, Part III 18*. Springer, 2015, pp. 234–241.
- [80] M. Caron, H. Touvron, I. Misra, H. Jégou, J. Mairal, P. Bojanowski, and A. Joulin, "Emerging properties in self-supervised vision transformers," in *Proceedings of the IEEE/CVF international conference on computer vision*, 2021, pp. 9650–9660.
- [81] X. Zhai, B. Mustafa, A. Kolesnikov, and L. Beyer, "Sigmoid loss for language image pre-training," in *Proceedings of the IEEE/CVF International Conference on Computer Vision*, 2023, pp. 11 975–11 986.
- [82] X. Yu, M. Xu, Y. Zhang, H. Liu, C. Ye, Y. Wu, Z. Yan, C. Zhu, Z. Xiong, T. Liang *et al.*, "Mvimnet: A large-scale dataset of multi-view images," in *Proceedings of the IEEE/CVF conference on computer vision and pattern recognition*, 2023, pp. 9150–9161.
- [83] C. Schuhmann, R. Beaumont, R. Vencu, C. Gordon, R. Wightman, M. Cherti, T. Coombes, A. Katta, C. Mullis, M. Wortsman *et al.*, "Laion-5b: An open large-scale dataset for training next generation image-text models," *Advances in Neural Information Processing Systems*, vol. 35, pp. 25 278–25 294, 2022.
- [84] A. Blattmann, T. Dockhorn, S. Kulal, D. Mendelevitch, M. Kilian, D. Lorenz, Y. Levi, Z. English, V. Voleti, A. Letts *et al.*, "Stable video diffusion: Scaling latent video diffusion models to large datasets," *arXiv preprint arXiv:2311.15127*, 2023.
- [85] J. Ho and T. Salimans, "Classifier-free diffusion guidance," *arXiv preprint arXiv:2207.12598*, 2022.
- [86] X. Pan, L. Dong, S. Huang, Z. Peng, W. Chen, and F. Wei, "Kosmog: Generating images in context with multimodal large language models," in *The Twelfth International Conference on Learning Representations*.
- [87] K. Song, Y. Zhu, B. Liu, Q. Yan, A. Elgammal, and X. Yang, "Moma: Multimodal llm adapter for fast personalized image generation," *arXiv preprint arXiv:2404.05674*, 2024.
- [88] Y. Zhang, Y. Song, J. Liu, R. Wang, J. Yu, H. Tang, H. Li, X. Tang, Y. Hu, H. Pan *et al.*, "Ssr-encoder: Encoding selective subject representation for subject-driven generation," in *Proceedings of the IEEE/CVF Conference on Computer Vision and Pattern Recognition*, 2024, pp. 8069–8078.
- [89] Q. Sun, Y. Cui, X. Zhang, F. Zhang, Q. Yu, Y. Wang, Y. Rao, J. Liu, T. Huang, and X. Wang, "Generative multimodal models are in-context learners," in *Proceedings of the IEEE/CVF Conference on Computer Vision and Pattern Recognition*, 2024, pp. 14 398–14 409.
- [90] M. Patel, S. Jung, C. Baral, and Y. Yang, "λ-eclipse: Multi-concept personalized text-to-image diffusion models by leveraging clip latent space," *arXiv preprint arXiv:2402.05195*, 2024.
- [91] X. Wang, S. Fu, Q. Huang, W. He, and H. Jiang, "Ms-diffusion: Multi-subject zero-shot image personalization with layout guidance," *arXiv preprint arXiv:2406.07209*, 2024.
- [92] A. Kirillov, E. Mintun, N. Ravi, H. Mao, C. Rolland, L. Gustafson, T. Xiao, S. Whitehead, A. C. Berg, W.-Y. Lo *et al.*, "Segment anything," *arXiv preprint arXiv:2304.02643*, 2023.
- [93] J. Xu, X. Liu, Y. Wu, Y. Tong, Q. Li, M. Ding, J. Tang, and Y. Dong, "Imagereward: Learning and evaluating human preferences for text-to-image generation," *arXiv preprint arXiv:2304.05977*, 2023.

## APPENDIX A EVALUATION BENCHMARKS

The full subject images used to evaluate single-subject customization are shown in Figure 18. These images are derived from the standard DreamBench [3] (the first three rows) and are further supplemented with more challenging cases in open domains, such as cartoon characters and buildings, for a more comprehensive evaluation than our conference version. For the first three rows of subject images, the corresponding editing prompts are listed in Table 9, which are also employed from the standard DreamBench benchmark.

For the last two rows of subject images, the corresponding editing prompts are listed below, created by users in real-application scenarios. The corresponding target real words for customization in each case are highlighted in blue.

- In the garden, the **little boy** was doodling, his paintbrush gently brushing over the paper.
- In the studio, the **woman** gently waved her animation brush and meticulously added colors to the canvas.
- The **little girl** sat in front of the piano, her nimble fingers lightly jumping, playing a melodious melody, immersed in the ocean of music.
- A **woman** is making ceramics in her own studio. She has a smile on her face and her hands are covered in the wet clay, shaping it carefully with a focused and calm expression.
- In the workshop, the **man** carefully adjusted the machine tool, wearing work clothes, and sweat slid down his forehead, fully focused on precise metal processing.
- A beautiful **Peking Opera actress**, dressed in gorgeous costumes and makeup, holding an ancient fan, turned around lightly and gently held the ancient fan with both hands, covering half of her face. There was a hint of mystery and expectation in her eyes. Shot on Polaroid film, the photo shows vivid colors and intricate details with a blurry background.
- Japanese animation, celluloid style, animation screenshots, fantasy world, magic fantasy, medieval times, night grassland. The **young magic apprentice**, holding a glowing magic bead, stood proudly in front of a shadow giant beast on the grassland.

editing prompts for non-live objects	editing prompts for live objects
"a in the jungle"	"a in the jungle"
"a in the snow"	"a in the snow"
"a on the beach"	"a on the beach"
"a on a cobblestone street"	"a on a cobblestone street"
"a on top of pink fabric"	"a on top of pink fabric"
"a on top of a wooden floor"	"a on top of a wooden floor"
"a with a city in the background"	"a with a city in the background"
"a with a blue house in the background"	"a with a blue house in the background"
"a on top of a purple rug in a forest"	"a on top of a purple rug in a forest"
"a with a wheat field in the background"	"a wearing a red hat"
"a with a tree and autumn leaves in the background"	"a wearing a santa hat"
"a with the Eiffel Tower in the background"	"a wearing rainbow scarf"
"a floating on top of water"	"a wearing a black top hat and a monocle"
"a floating in an ocean of milk"	"a in a checf outfit"
"a on top of green grass with sunflowers around it"	"a in a firefighter outfit"
"a on top of a mirror"	"a in a police outfit"
"a on top of the sidewalk in a crowded street"	"a wearing pink sunglasses"
"a on top of a dirt road"	"a wearing a yellow shirt"
"a on top of a white rug"	"a in a purple wizard outfit"
"a red "	"a red "
"a purple "	"a purple "
"a shiny "	"a shiny "
"a wet "	"a wet "
"a cube shaped "	"a cube shaped "

TABLE 9: Editing prompt list for quantitative evaluation on single subject customization. For our proposed RealCustom++, "" is replaced with the super-category of the given subject, while for other methods of previous pseudo-word paradigm, "" is replaced with the learned pseudo word, i.e., S\*.

- Realism, Unreal Engine, cinematic feel, exaggerated lighting, cyberpunk, future world, advanced technology, city with neon lights at night, vehicle chase scene, capable woman with short blue hair, wearing high-tech tights, jumping from the roof of the car to the roof of another car.
- The city tower with bright lights at night.
- A boy dresses in a Christmas style is lying on the sofa, with close-up shots, diagonal angles, and physical photography.
- A pavilion built in the mountains, with a waterfall beside it.
- Otter is playing with toys in the water.
- The hippopotamus in the zoo is eating watermelon.
- An Asian woman is wearing the T-shirt walking in the jungle.
- A koala wearing a mortarboard cap is reading a difficult book under a tree.
- The boy is singing on the beach wearing a black punk denim jacket, blue jeans, and heart-shaped sunglasses.
- On the beach, a girl is building a complex sand castle with a joyful smile on her face.
- In a busy market, a girl is bargaining with a vendor.
- Donald Duck is singing on stage.
- Stitch is singing a song in punk clothes.

The subject images and corresponding editing prompts for multiple-subjects customization evaluation are listed in Figure 19.

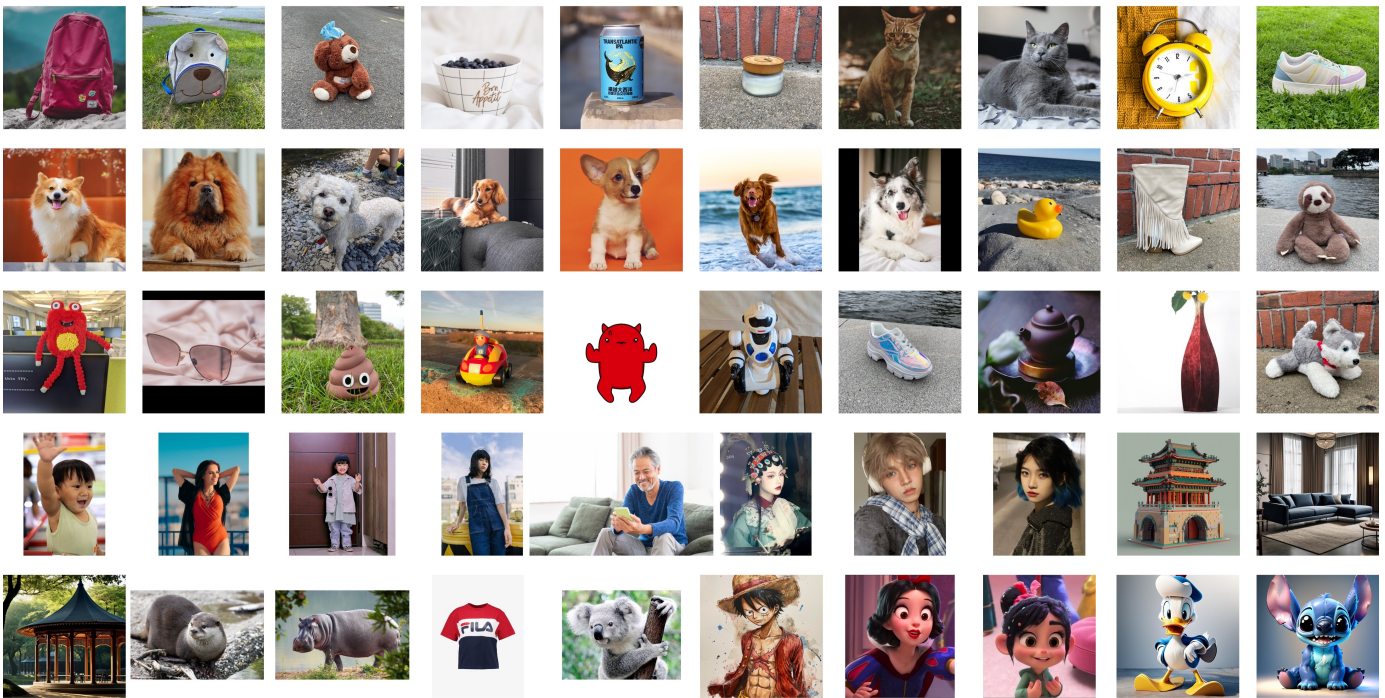


Fig. 18: The subject images for single-subject customization evaluation, which are derived from the standard DreamBench [3] (the first three row) and are further supplemented with more challenging cases in open domains, such as cartoon characters and buildings, for a more comprehensive evaluation than our conference version.





















		<ul style="list-style-type: none"> <li>(1) The <b>boy</b> is wearing the <b>coat</b>, playing the piano on the stage.</li> <li>(2) The <b>boy</b> is running through the park, his coat flapping in the wind. The sun is setting, casting a golden hue over the scene.</li> <li>(3) In the bustling city, the <b>boy</b> stands at the bus stop, his <b>coat</b> buttoned up tightly against the cold.</li> </ul>
		<ul style="list-style-type: none"> <li>(1) The <b>dog</b> is wearing a <b>pair of sunglasses</b> on the beach.</li> <li>(2) At the outdoor concert, the <b>dog</b> sits calmly with a <b>pair of sunglasses</b>, enjoying the music and the crowd.</li> <li>(3) The <b>dog</b>, donning a <b>pair of sunglasses</b>, explores an alien planet, sniffing at the strange, glowing flora.</li> </ul>
		<ul style="list-style-type: none"> <li>(1) The <b>girl in white T-shirt and brown skirt</b> is playing chess with <b>Stitch</b> in the park.</li> <li>(2) The <b>girl in white T-shirt and brown skirt</b> is exploring a magical forest with <b>Stitch</b>, discovering glowing plants and mystical creatures.</li> <li>(3) At the science fair, the <b>girl in white T-shirt and brown skirt</b> is conducting an experiment with <b>Stitch</b>, mixing colorful chemicals in test tubes.</li> </ul>
		<ul style="list-style-type: none"> <li>(1) The <b>girl</b> is playing the <b>red guitar</b> in the room.</li> <li>(2) The <b>girl</b> sits on the rooftop at sunset, playing the <b>red guitar</b> as the city lights begin to twinkle.</li> <li>(3) The <b>girl</b>, holding the <b>red guitar</b>, poses for a photo shoot in a sunlit studio, capturing her passion for music.</li> </ul>
		<ul style="list-style-type: none"> <li>(1) The <b>dog</b> is sitting on the ground, with the <b>pavilion</b> in the background.</li> <li>(2) In the park, the <b>dog</b> rests under the shade of the <b>pavilion</b>, panting softly after a long walk.</li> <li>(3) At the lakeside, the <b>dog</b> splashes in the water while the <b>pavilion</b> reflects on the calm surface.</li> </ul>
		<ul style="list-style-type: none"> <li>(1) The <b>young magic apprentice</b> is holding a shining magic pearl, and an <b>ancient tower</b> is in the background.</li> <li>(2) The <b>young magic apprentice</b>, riding a broomstick, flies past the <b>ancient tower</b> under the moonlit sky.</li> <li>(3) The <b>young magic apprentice</b>, accompanied by a mystical creature, explores the ruins surrounding the <b>ancient tower</b>.</li> </ul>
		<ul style="list-style-type: none"> <li>(1) The <b>otter</b> is sitting on the <b>fancy pink sofa</b>, playing with many toys in the room.</li> <li>(2) The <b>otter</b>, resting on the <b>fancy pink sofa</b>, gazes curiously at the aquarium across the room.</li> <li>(3) The <b>otter</b>, perched on a tree branch, looks down at the <b>fancy pink sofa</b> placed in the garden below.</li> </ul>
		<ul style="list-style-type: none"> <li>(1) The <b>little raccoon</b> is driving the <b>motorcycle</b> on the road.</li> <li>(2) As the sun sets, the <b>little raccoon</b> parks the <b>motorcycle</b> at a scenic overlook, taking in the breathtaking view.</li> <li>(3) At the countryside fair, the <b>little raccoon</b> shows off the <b>motorcycle</b> to a curious crowd, explaining its features.</li> </ul>
		<ul style="list-style-type: none"> <li>(1) The <b>little girl</b> was walking along a cobblestone path with the <b>dog</b>, the weather is nice.</li> <li>(2) The <b>little girl</b>, wearing a sunhat, reads a book while sitting on the cobblestone path, with the <b>dog</b> lying next to her.</li> <li>(3) In the garden, the <b>little girl</b> picks flowers while the <b>dog</b> sniffs around the cobblestone path.</li> </ul>
		<ul style="list-style-type: none"> <li>(1) The <b>beautiful girl</b> is building a complex sand castle with <b>Winnie</b> on the beach.</li> <li>(2) The <b>beautiful girl</b>, holding a bouquet of flowers, poses for a photo with <b>Winnie</b> in front of a picturesque landscape.</li> <li>(3) The <b>beautiful girl</b> is painting a portrait of <b>Winnie</b> in the garden, surrounded by blooming flowers.</li> </ul>

Fig. 19: The subject images and corresponding editing prompts for multiple-subject customization evaluation are shown. The target real words for each given subject are highlighted in color.